Implications of 21st Century Climate Change for the Hydrology of Washington State

Article *in* Climatic Change · September 2010

DOI: 10.1007/s10584-010-9855-0

Climatic Change (2010) 102:225–260
DOI 10.1007/s10584-010-9855-0

Implications of 21st century climate change for the hydrology of Washington State

Marketa M. Elsner · Lan Cuo · Nathalie Voisin · Jeffrey S. Deems · Alan F. Hamlet · Julie A. Vano · Kristian E. B. Mickelson · Se-Yeun Lee · Dennis P. Lettenmaier

Received: 4 June 2009 / Accepted: 23 March 2010 / Published online: 4 May 2010

Abstract Pacific Northwest (PNW) hydrology is particularly sensitive to changes in climate because snowmelt dominates seasonal runoff, and temperature changes impact the rain/snow balance. Based on results from the Fourth Assessment Report of the Intergovernmental Panel on Climate Change (IPCC AR4), we updated previous studies of implications of climate change on PNW hydrology. PNW 21st century hydrology was simulated using 20 Global Climate Models (GCMs) and 2 greenhouse gas emissions scenarios over Washington and the greater Columbia River watershed, with additional focus on the Yakima River watershed and the Puget Sound which are particularly sensitive to climate change. We evaluated projected changes in snow water equivalent (SWE), soil moisture, runoff, and streamflow for A1B and B1 emissions scenarios for the 2020s, 2040s, and 2080s. April 1 SWE is projected to decrease by approximately 38–46% by the 2040s (compared with the mean over water years 1917–2006), based on composite scenarios of B1 and A1B,

M. M. Elsner (✉) · A. F. Hamlet · D. P. Lettenmaier
Center for Science in the Earth System, Climate Impacts Group, University of Washington,
Box 355672, Seattle, WA 98195-5672, USA
e-mail: mmcguire@uw.edu

L. Cuo
Australia Commonwealth Scientific and Industrial Research Organization (CSIRO),
37 Graham Road, Highett, VIC 3190, Australia

N. Voisin · A. F. Hamlet · J. A. Vano · S.-Y. Lee · D. P. Lettenmaier
Department of Civil and Environmental Engineering, University of Washington,
Box 352700, Seattle, WA 98195-2700, USA

J. S. Deems
National Snow and Ice Data Center, 449 UCB University of Colorado,
Boulder, CO 80309-0449, USA

K. E. B. Mickelson
US Army Corps of Engineers, Seattle District, P.O. Box 3755,
Seattle, WA 98124-3755, USA

respectively, which represent average effects of all climate models. In three relatively warm transient watersheds west of the Cascade crest, April 1 SWE is projected to almost completely disappear by the 2080s. By the 2080s, seasonal streamflow timing will shift significantly in both snowmelt dominant and rain–snow mixed watersheds. Annual runoff across the State is projected to increase by 2–3% by the 2040s; these changes are mainly driven by projected increases in winter precipitation.

1 Introduction

The Fourth Assessment Report (AR4) of the Intergovernmental Panel on Climate Change (IPCC) states that warming of Earth's climate is unequivocal and that anthropogenic use of fossil fuels has contributed to increasing carbon dioxide concentrations and thereby warming of the atmosphere (IPCC 2007). The hydrology of the Pacific Northwest (PNW—which typically includes the Columbia River basin and watersheds draining to the Oregon and Washington coasts) is particularly sensitive to changes in climate because of the role of mountain snowpack on the region's rivers. In this paper, we utilize archived climate projections from the IPCC AR4 to evaluate impacts on PNW regional hydrology, with focus on Washington (Fig. 1).

Washington is partitioned into two distinct climatic regimes by the Cascade Mountains. The west side of the Cascades on average receives approximately 1,250 mm of precipitation annually, while the east side receives slightly more than one-quarter of this amount. Washington's watersheds, like most in the western USA, rely on cool season precipitation (defined as October through March) and resulting snowpack to sustain warm season streamflows (defined as April through September). Most of the annual precipitation in the Cascades falls during the cool season (Hamlet and Lettenmaier 1999). A changing climate affects the balance of precipitation falling as rain and snow and therefore the timing of streamflow over the course of the year. Figure 2 illustrates simulated historical mean annual runoff over water years 1917–2006 using the variable infiltration capacity (VIC) hydrologic model (further described below) and shows the importance of the State's mountainous regions with respect to water supply for various natural resources.

Small changes in temperature can strongly influence the balance of precipitation falling as rain and snow, depending on a watershed's location, elevation, and aspect. Washington, and the PNW as a whole, is often characterized as having three runoff regimes: snow-melt dominant, rain dominant, and transient (Hamlet and Lettenmaier 2007). In snowmelt dominant watersheds, much of the winter precipitation is stored in the snowpack, which melts in the spring and early summer resulting in low streamflow in the cool season and peak streamflow in late spring or early summer (May–July). Rain dominant watersheds are typically located at lower elevations and predominantly on the west side of the Cascades. Streamflow in these watersheds peaks in the cool season, roughly in phase with peak precipitation (usually November through January). Transient watersheds are characterized as mixed rain–snow due to their mid-range elevation and where winter temperatures fluctuate around freezing. These watersheds receive some snowfall, some of which melts in the cool season and some of which is stored over winter and melts as seasonal temperatures increase. Rivers draining these watersheds typically experience two streamflow peaks: one in winter coinciding with seasonal maximum precipitation,

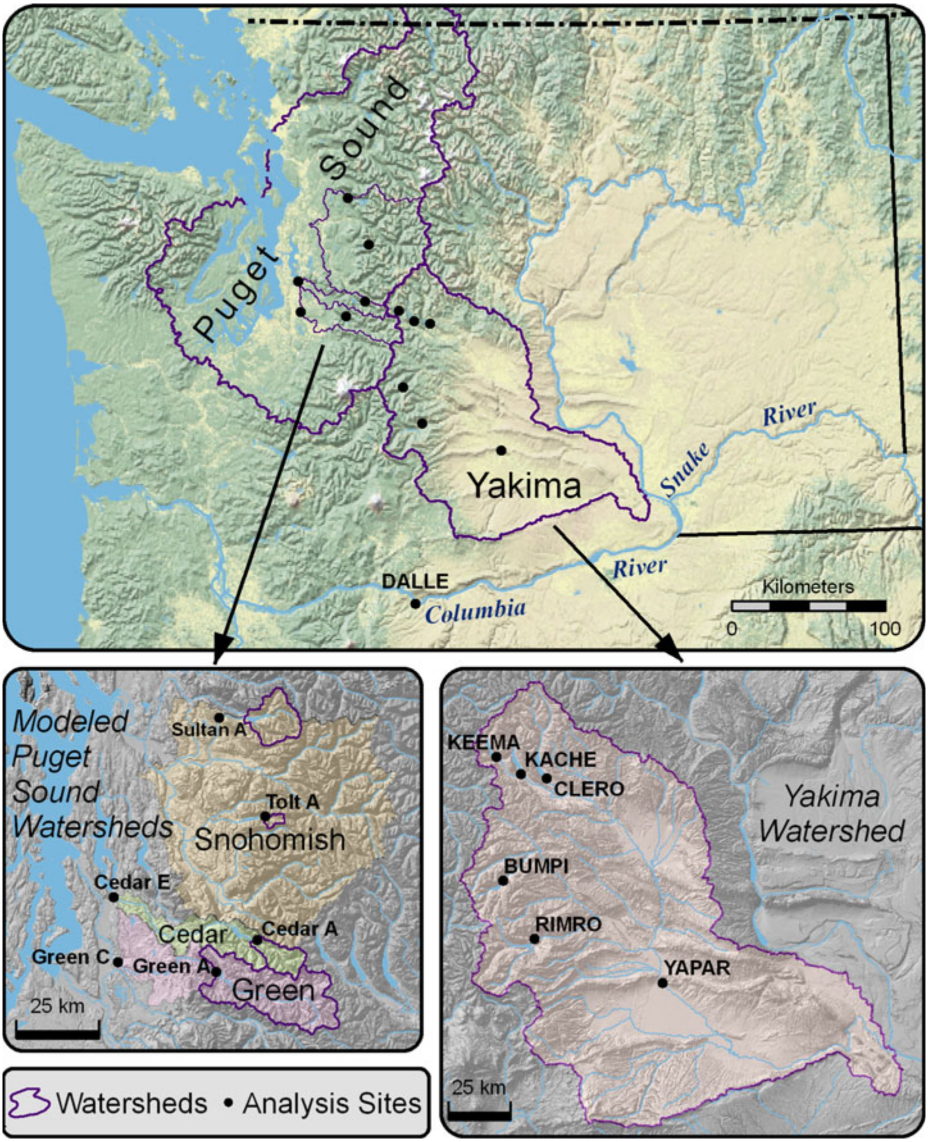

Fig. 1 Overview figure of Washington State, Puget Sound and Yakima case study watersheds, and significant analysis locations. Figure: Robert Norheim

and another in late spring or early summer when water stored in snowpack melts. Hydrographs of simulated average historic streamflow, which are representative of the three watershed types, are shown in Fig. 3. Hydrologic simulations from which these hydrographs were developed are fully described in Section 2.2 below. The Chehalis River, which drains to the Washington coast, is a characteristic rain dominant watershed, while the Yakima River, which drains to the Columbia River, is a characteristic transient watershed, and the Columbia River as a whole, which drains

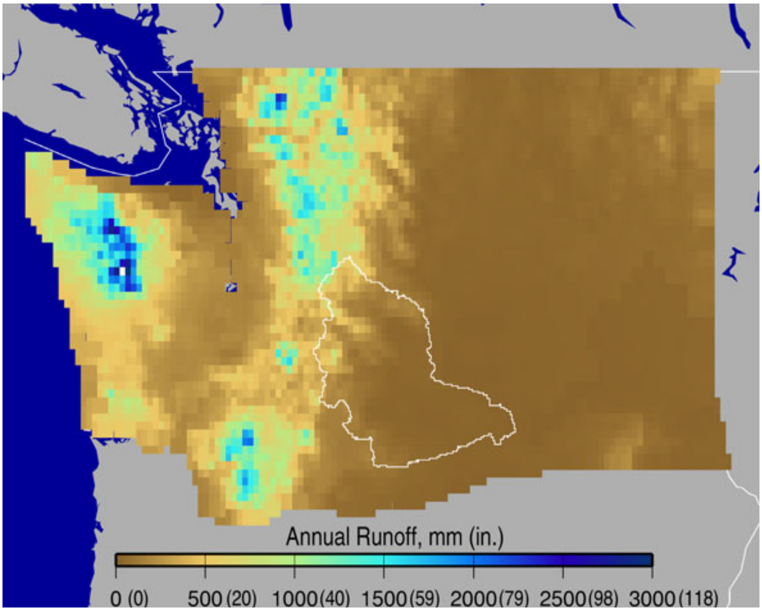

Fig. 2 Simulated mean annual runoff over Washington State by the variable infiltration capacity (VIC) model over the historic period from 1917–2006 (water years)

from mountainous regions in mainly Canada, Idaho, Oregon, and Washington, is a characteristic snowmelt dominant watershed.

Previous studies have presented metrics which can be used to define watershed type. Barnett et al. (2005) suggested a metric defined as the ratio of peak snow water equivalent (SWE) to total cool season (October–March) precipitation. SWE is defined as the liquid water content of the snowpack. Barnett et al. (2008) also showed that SWE to precipitation ratios have been declining in the historic record due to observed warming, and that these changes are predominantly related to human influence on the climate. Regionally, Hamlet and Lettenmaier (2007) characterized the three types of watersheds over the Pacific Northwest by temperature. Snowmelt dominant watersheds have average winter temperatures of less than −6°C, while completely rain dominant watersheds have average temperatures above 5°C. Their analysis explored changes in flood characteristics over basins of varying scale for these watershed categories. Mantua et al. (2010) also applied the SWE to precipitation ratio metric to the hydrologic unit code (HUC) 4 regions in the PNW as a means to catalogue high-disturbance areas. In Fig. 4, we show the peak SWE to precipitation ratio computed for 1/16th degree grid cells over Washington. Rain-dominant regions generally have ratios less than 0.1; transient regions are in the range of about 0.1–0.4; and, snowmelt dominant regions generally have ratios greater than 0.4 (see additional figures and discussion in Mantua et al. 2010). Figure 4 shows the locations of the stream gauges from which the hydrographs presented in Fig. 3 are derived. It also illustrates that the urban water supply systems for the State's major metropolitan areas in the Puget Sound (including watersheds of the Cedar River, Green River, South Fork [SF] Tolt River, and Sultan River) and the agriculturally rich Yakima River watershed are located in transient regions. As shown in accompanying papers

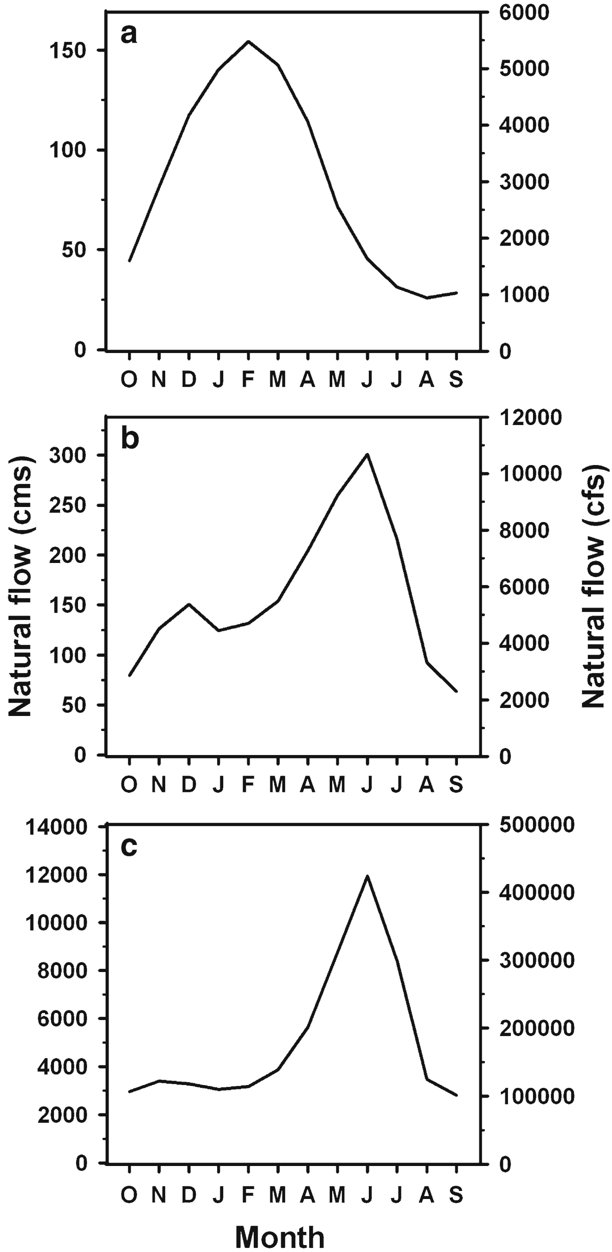

Fig. 3 Simulated monthly historic streamflow hydrographs for three representative watershed types in Washington: **a** rain dominant (Chehalis River at Porter), **b** transient rain–snow (Yakima River at Parker), and **c** snowmelt dominant (Columbia River at The Dalles). Hydrographs shown are monthly averages of simulated daily streamflow from the VIC model for water years 1917–2006

by Vano et al. (2010a, b), shifts in seasonal streamflow toward higher winter flow and lower summer flow have strong implications for water management in these regions. This paper focuses on hydrologic impacts of climate change on Washington and on the sensitive transient watersheds of the Puget Sound and Yakima River, which are the basis for the water management assessments by Vano et al. (2010a, b, respectively).

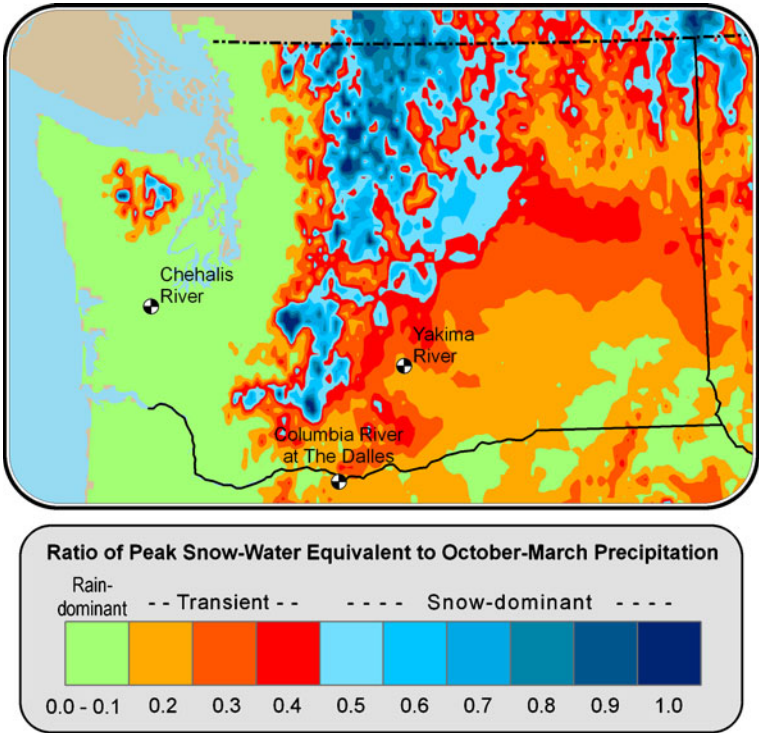

Fig. 4 The average ratio of peak VIC model simulated snow water equivalent (SWE) to October–March precipitation for the historical period (water years 1917–2006). Figure: Robert Norheim

2 Approach and methods

We applied a range of climate change projections from the IPCC AR4 (IPCC 2007) to generate hydrologic model simulations and to evaluate the impact of climate change broadly on the hydrology of Washington State, with additional focus on the Yakima River watershed (Vano et al. 2010a), which supports irrigation of high-valued crops such as orchards, and those Puget Sound watersheds that supply water to a majority of the state's population (Vano et al. 2010b). We performed the hydrologic simulations using the VIC macroscale hydrology model (Liang et al. 1994; Nijssen et al. 1997) at 1/16th degree latitude by longitude spatial resolution over the greater Columbia River watershed (approximately 5 by 6 km grid cells). This approach allowed us to evaluate changes not only in Washington, but also in watersheds outside the state boundary that affect hydropower energy production within the larger Pacific Northwest region (Hamlet et al. 2010). We also applied DHSVM, the Distributed Hydrology Soil and Vegetation Model (Wigmosta et al. 1994), at 150 meter spatial resolution over the Puget Sound watersheds. We used these models to explore the sensitivity of runoff to changes in precipitation and temperature over our focus regions. We then evaluated implications of projected changes in snowpack (specifically snow water equivalent) and soil moisture (defined by depth of water in the soil column) over the same domains.

2.1 Hydrologic simulations

Studies of climate change impacts on regional hydrology are becoming increasingly common (Maurer 2007; Maurer and Duffy 2005; Hayhoe et al. 2007; Christensen and Lettenmaier 2007; Christensen et al. 2004; Payne et al. 2004; Van Rheenen et al. 2004; Miller et al. 2003; among others). Many of these studies use a scenario approach which evaluates projections of hydrological variables, like streamflow, using a hydrology model forced with downscaled ensembles of projected climate from global climate models (GCMs). These future climate simulations are then compared with a baseline hydrological simulation using historical climate (see e.g. Christensen and Lettenmaier 2007; Maurer 2007; Hayhoe et al. 2007; among others). This approach is sometimes termed "off-line" forcing of a hydrological model, because it does not directly represent feedbacks between the land surface and climate system. An alternative approach, based on regional climate models, represents land-atmosphere feedbacks; however, complications arise due to bias in the climate model simulations (see Wood et al. 2004 for a detailed discussion), and computational requirements which generally preclude the use of multi-model ensemble methods. For this reason, we used the off-line simulation approach.

We used climate change scenarios to force two hydrology models—the VIC Model (Liang et al. 1994, 1996; Nijssen et al. 1997) and DHSVM (Wigmosta et al. 1994). The VIC model is a macroscale model, meaning it is intended for application to relatively large distributed areas, typically ranging from 10,000 km^2 or so, up to continental and even global scales. A key underlying model assumption is that sub-grid scale variability (in vegetation, topography, soil properties, etc.) can be parameterized, rather than represented explicitly. We evaluated VIC model simulations over all of Washington (and over the entire PNW), including the Yakima River watershed, which covers 15,850 km^2.

DHSVM is an explicitly distributed hydrology model, intended for application at much higher spatial resolution (and hence to smaller areas) than VIC. In this study, we applied DHSVM to relatively small river basins flowing to the Puget Sound at a 150 m spatial resolution. These watersheds range from 52–1,055 km^2 in area. Both VIC and DHSVM are described in more detail below.

2.1.1 Variable infiltration capacity (VIC) model

The VIC model (Liang et al. 1994, 1996; Nijssen et al. 1997) has been used to assess the impact of climate change on U.S. hydrology in a number of previous studies. Hamlet and Lettenmaier (1999) studied the implications of GCM projections from the second IPCC assessment (1995) over the Columbia River watershed. Following the third IPCC Assessment Report (2001), Payne et al. (2004) studied climate change effects on the Columbia River, Christensen et al. (2004) studied effects on the Colorado River, and Van Rheenen et al. (2004) studied effects on California. Similarly, several recent studies involved implementation of the VIC model to analyze the effects of IPCC AR4 projections on hydrologic systems: Vicuna et al. (2007) and Maurer (2007) in California, Christensen and Lettenmaier (2007) on the Colorado River, and Hayhoe et al. (2007) on the northeastern U.S.

Although predictions of winter precipitation changes over the PNW have differed somewhat among recent IPCC reports (the 1995 report suggests an increase, whereas the 2001 report indicates only modest changes), all previous assessments have

Table 1 Summary statistics of model calibration and validation for the Variable Infiltration Capacity (VIC) model in units of cubic meters per second

Watersheds (gage)	Annual mean for calibration period			N–S model efficiency	
	Nat. (m3/s)	Sim. (m3/s)	Rel. error (%)	Calibration (monthly)	Validation (monthly)
Yakima (12505000)					
Calibration period (1986–2000)	127.7	157.6 (134.8)	23 (5.6)	0.56 (0.72)	0.64 (0.89)
Validation period (1971–1985)					
Columbia (14105700)					
Calibration period (1986–1998)	5,386	5,321	1.2	0.87	0.84
Validation period (1970–1985)					

The relative error is defined as the ratio of the difference between mean annual simulated flow (sim.) and mean annual observed natural flow (nat.) to the mean annual observed natural flow. The Nash Sutcliffe efficiency is a coefficient which is commonly used to define hydrologic predictive power, where a coefficient of one is a perfect match between simulated and observed natural flow. Values in parentheses indicate statistics after bias correction

projected warmer temperatures leading to projections of reduced snowpack, and hence a transition from spring to winter runoff (Hamlet and Lettenmaier 1999; Payne et al. 2004). Other impacts common to previous studies of hydrological impacts of climate change in the PNW include earlier spring peak flow and lower summer flows.

In this paper, we used GCM simulations archived for the IPCC AR4 and increased the spatial resolution of the hydrological model over the PNW from 1/8th degree (used in all previous studies cited above) to 1/16th degree. An historical input data set including daily precipitation, maximum and minimum daily temperature, and windspeed was developed for this study at 1/16th degree spatial resolution and its unique features are described in Section 2.2.1. Model calibration at routed streamflow locations included the use of initial parameters for the 1/8th degree VIC model (Matheussen et al. 2000), transferred to the 1/16th degree model. These parameters were evaluated at 1/16th resolution at two calibration locations (Table 1). Model calibration and validation statistics for the VIC model used in this study are provided in Table 1 and include relative error in mean annual streamflow and Nash Sutcliffe efficiencies. A well calibrated model typically yields a relative error less than 10% and a Nash Sutcliffe efficiency higher than 0.7 (Liang et al. 1996; Nijssen et al. 1997). Calibration and validation periods were chosen to include a range of streamflow conditions with which to test model performance. Although streamflow error statistics for the Yakima River watershed were larger than desirable (perhaps in part as a result of discrepancies in the naturalized streamflow data to which the model was calibrated), subsequent application of a bias correction, consistent with Wood et al. (2002) and Snover et al. (2003), removes most of the model bias (error statistics reported in Table 1).

Variables other than streamflow (e.g. simulated SWE or soil moisture) were not used to further constrain model parameters. However, previous studies indicate that the model successfully simulates grid level processes. Mote et al. (2005) validated the sensitivity of the VIC snow model to changing temperature and precipitation in historical records, while Andreadis et al. (2009) compared VIC-simulated SWE with observations to show that the model captures observed snow accumulation and ablation reasonably well in varied forested terrain. Maurer et al. (2002) showed that VIC-simulated historical soil moisture was comparable to available observations. Hamlet and Lettenmaier (2007) showed that despite considerable bias in simulated absolute values, the persistent relationships between the mean annual flood and the extremes (e.g. 100-year flood) across a wide range of climatic conditions indicate the model's ability to capture the effects of observed changes in climate. In addition to increasing the VIC model resolution for this study, the number of GCMs from which the ensembles are formed was increased substantially relative to previous studies.

We also adapted the model to allow output of potential evapotranspiration (PET) for each model grid cell. PET is the amount of water that would be transpired by vegetation, provided unlimited water supply, and is often used as a reference value of land surface water stress in characterizations of climate interactions with forest processes (e.g., Littell et al. 2010). PET is calculated in the VIC model using the Penman–Montieth approach (Liang et al. 1996) and the user may choose to output PET of natural vegetation, open water PET, as well as PET of certain reference agricultural crops.

2.1.2 Distributed hydrology soil vegetation model (DHSVM)

DHSVM was originally designed for application to mountainous forested watersheds, and includes explicit representations of the effects of forest vegetation on the water cycle. In particular, the model captures the role of vegetation as it intercepts liquid and solid precipitation, and the effect snow accumulation and ablation under forest canopies. Early applications of the model addressed how forest harvest affected flood frequency in the PNW (Bowling et al. 2000; La Marche and Lettenmaier 2001; Bowling and Lettenmaier 2001). The model represents runoff primarily via the saturation excess mechanism and explicitly represents the depth to water table at each model pixel, which has typically ranged from 10–200 m in past applications of the model (in our application to the Puget Sound basins, we used 150 m spatial resolution).

Some DHSVM model parameterizations are similar to those in Topmodel (Beven and Kirkby 1979); a key difference is the explicit, rather than statistical representation of downslope redistribution of moisture in the saturated zone. In addition to its representation of the water table and downslope redistribution of moisture, DHSVM represents the land surface energy balance (in a manner similar to VIC), unsaturated soil moisture movement, saturation overland flow, and snowmelt and accumulation. DHSVM simulates snow accumulation and ablation, using the same snow model used by VIC, which is described by Cherkauer et al. (2003) and Andreadis et al. (2009). In brief, it uses a two-layer snow algorithm, in which the top layer is used to solve an energy balance with the atmosphere, including effects of vegetation cover, while the bottom layer is used as storage to simulate deeper snowpack. Although VIC and DHSVM use virtually identical snow models, model structure may play a significant role in the results. The VIC model does not represent slope and aspect effects, whereas DHSVM does. Furthermore, DHSVM includes a representation of canopy closure (hence clearings between trees) whereas VIC does not. These differences are likely to be largest for point or small area comparisons, and are likely reduced when averaging over large areas.

Using a 150 m resolution digital elevation model (DEM) as a base map (US Department of Interior/US Geological Survey, http://seamless.usgs.gov), DHSVM explicitly accounts for soil and vegetation types and stream channel network and morphology. Wigmosta and Lettenmaier (1999) and Wigmosta et al. (1994) provide a detailed description of the model. The model also uses a soil class map based on the STATSGO soil map produced by the U.S. Department of Agriculture. The land cover map was derived from Alberti et al. (2004). Although not addressed by this study, the impacts of vegetation change on hydrology have previously been evaluated by Matheussen et al. (2000) over the Columbia River watershed and Cuo et al. (2009) over the Puget Sound drainages. Generally, the magnitude of the impacts they attribute to vegetation change over the last century relative to the changes we attribute to future climate change are modest at the seasonal scale, but can be comparable on an annual basis. The forested areas studied in the two above-mentioned papers are representative of those parts of the State that have the highest runoff. While land cover conversions to and from cropland have the potential to result in substantial changes in runoff, their effects at a statewide or watershed scale most likely are small, primarily because most croplands are in areas of low precipitation and runoff.

The model is forced by climate inputs including precipitation and temperature, (at daily or shorter time steps), downward solar and longwave radiation, surface

Table 2 Summary statistics of model calibration and validation for the Distributed Hydrology Soil and Vegetation Model (DHSVM) in units of cubic meters per second

Watersheds (gage)	Annual mean for calibration period			N–S model efficiency		
	Nat. (m^3/s)	Sim. (m^3/s)	Rel. error (%)	Calib. (daily)	Calib. (monthly)	Valid. (monthly)
Snohomish (12141300)						
Calibration period (1993–2002)	35.5	36.1	2	0.50	0.79	0.75
Validation period (1983–1993)						
Cedar (12115000)						
Calibration period (1982–1992)	6.85	6.18	−10	0.61	0.81	0.81
Validation period (1992–2002)						
Green (12104500)						
Calibration Period (1973–1983)	9.79	9.76	0	0.54	0.72	0.71
Validation Period (1983–1993)						
Tolt (12147600)						
Calibration period (1983–1993)	1.52	1.39	−9	0.45	0.70	0.75
Validation period (1993–2002)						

The relative error is defined as the ratio of the difference between mean annual simulated flow (sim.) and mean annual observed natural flow (nat.) to the mean annual observed natural flow. The Nash Sutcliffe efficiency is a coefficient which is commonly used to define hydrologic predictive power, where a coefficient of one is a perfect match between simulated and observed natural flow humidity, and wind speed. Using the historical 1/16th degree dataset developed for the VIC model (described below) and procedures developed by Nijssen et al. (2001), daily forcings were disaggregated to 3-hour intervals as described in detail by Cuo et al. (2008), who applied DHSVM to all Puget Sound drainages. Additionally, forcings at 1/16th degree were interpolated to 150 m resolution using a Cressman interpolation scheme. Model calibration and validation statistics for the DHSVM used in this study are provided in Table 2. Similar to VIC, a well calibrated DHSVM model typically yields a relative error less than 10% and a Nash Sutcliffe efficiency higher than 0.7 (Wigmosta et al. 1994; Leung et al. 1996). Calibration and validation periods were chosen to include a range of streamflow conditions with which to test model performance.

2.2 Model input variables

2.2.1 Historical inputs

Both VIC and DHSVM require as forcing variables precipitation (Prcp) and temperature at a sub-daily time step, as well as downward solar and longwave radiation, surface wind, and vapor pressure deficit. All simulations described in this paper are based on a 1/16th degree spatial resolution data set of daily historical Prcp and daily temperature maxima and minima (Tmax, Tmin) developed from observations following methods described in Maurer et al. (2002) and Hamlet and Lettenmaier (2005), adapted as described below. Forcing variables other than daily precipitation and temperature maxima and minima are derived from the daily temperature range or mean temperature following methods outlined in Maurer et al. (2002). One exception is surface wind. Daily wind speed values for 1949–2006 were downscaled from National Centers for Environmental Prediction-National Center for Atmospheric Research (NCEP-NCAR) reanalysis products (Kalanay et al. 1996). For years prior to 1949, daily wind speed climatology was derived from the 1949–2006 reanalysis.

We used the National Climatic Data Center Cooperative Observer (Co-Op) network and Environment Canada (EC) daily station data as the primary sources for precipitation and temperature values. We used a method described by Hamlet and Lettenmaier (2005) that corrects for temporal inhomogeneities in the raw gridded data using a set of temporally consistent and quality controlled index stations from the US Historical Climatology Network (HCN) and the Adjusted Historical Canadian Climate Database (AHCCD) data. This approach assures that no spurious trends are introduced into the gridded historical data as a result of inclusion of stations with records shorter than the length of the gridded data set. The data are adjusted for orographic effects using the PRISM (Daly et al. 1994, 2002) climatology (1971–2001) following methods outlined in Maurer et al. (2002).

Daily station data from 1915 to 2006 were processed as in Hamlet and Lettenmaier (2005), but using only Co-Op, EC, HCN, and AHCCD stations within a 100 km buffer of the domain. Quality control flags included in the raw Co-Op data set for each recorded value were used to ensure accuracy and to temporally redistribute "accumulated" Prcp values. We used the Symap algorithm (Shepard 1984; as per Maurer et al. 2002) to interpolate Co-Op/EC station data to a 1/16th degree.

We then adjusted the daily Prcp, Tmax, and Tmin values for topographic influences by scaling the monthly means to match the monthly PRISM climate normals from 1970–2000. In the temperature rescaling method used for this study, Tmax and Tmin were adjusted by the same amount to avoid introducing a bias into daily mean temperatures and the daily temperature range. First, the average of the Tmax and Tmin values were computed for each of the monthly PRISM and monthly mean Co-Op time series. The difference between these values was applied as an offset to the average of the daily Tmax and Tmin in the appropriate month, thereby explicitly preserving the daily temperature range. For days where Tmin exceeds Tmax due to interpolation errors in the initial regridding step, we offset the average of these inverted Tmax and Tmin values and applied a climatological daily range from PRISM Tmax and Tmin.

The historical datasets developed for this study extend from January 1915 to December 2006. Results from historical simulations presented in this study and the period to which projected hydrologic scenarios are compared extend from October 1916 to September 2006 (water years 1917 to 2006) to allow for sufficient hydrologic model spinup.

2.2.2 Regional climate change projections

As part of the IPCC AR4, results from a common set of simulations of twenty-first century climate were archived from 21 GCMs (Mote and Salathé 2010), using greenhouse gas emissions scenarios as summarized in the IPCC's Special Report on Emissions Scenarios (SRES) (Nakićenović and Swart 2000). Simulations were archived predominantly for three SRES emissions scenarios (A1B, B1, and A2) for most of the 21 GCMs, with A2 following the highest trajectory for future CO_2 emissions at the end of the 21st century. We focus on A1B and B1 emission scenarios because these were simulated by the most GCMs and our study focuses on mid-century change, at which point none of the scenarios is consistently the highest. Following Mote and Salathé (2010), we used output from 20 of the GCMs for which monthly gridded precipitation, temperature, and other variables were archived for SRES emissions scenario A1B, and 19 for which the same variables were archived for emissions scenario B1. Mote and Salathé (2010) summarize the GCM predictions of twenty-first century precipitation and temperature over the Pacific Northwest, and evaluate performance of the GCMs in reconstructing 20th century climate. No single GCM 20th century simulation was preferred when evaluated using multiple performance criteria, suggesting that use of a multimodel ensemble for evaluating climate change impacts is preferable to attempts to identify a "best" model or models. The spatial resolution of the 20 models varies, but is generally about three degrees latitude by longitude; therefore, we downscaled the climate model output to the spatial resolution of a regional hydrology model as described below.

2.2.3 Downscaling procedures

In general, the GCM output is at too coarse a spatial resolution to be meaningful for hydrological studies. Therefore, we downscaled the GCM output to 1/16th degree spatial resolution and applied a delta method approach to develop climate change scenarios with which to evaluate impacts (see e.g. Hamlet and Lettenmaier 1999; Snover et al. 2003). In the delta method, projected changes in precipitation and temperature, as determined by GCM simulations, are applied to the historical record at the resolution of hydrologic models. We used regional projected monthly changes derived from a total of 39 climate ensembles (described in Section 2.2.2). We performed hydrologic simulations using the historical record perturbed by these monthly changes and then evaluated impacts of climate change on a number of hydrologic variables.

There are three previously established ways of developing climate change scenarios based on GCM output, downscaled to the appropriate spatial resolution required for off-line hydrologic simulations. As noted above, the delta method simply applies monthly changes in temperature and precipitation from the GCM to historical inputs or inputs derived from historical data, which in turn are used to force the hydrological model in the same way that simulations using historical forcings are performed. For instance, this approach was used by Hamlet and Lettenmaier (1999) in their study of the Columbia River watershed. The second approach uses transient projections of future climate from GCMs statistically downscaled to the spatial resolution of a hydrological model and from a monthly to daily time step, using archived GCM model output from sources such as the World Climate Research Programme's (WCRP's) Coupled Model Intercomparison Project phase 3 (CMIP3) multi-model dataset. This approach was used by Christensen et al. (2004) and Christensen and Lettenmaier (2007) in the Colorado River watershed, Van Rheenen et al. (2004), Maurer and Duffy (2005) in the Sacramento and San Joaquin watersheds of California, Payne et al. (2004) in the Columbia River watershed, and Hayhoe et al. (2007) over the northeastern U.S. All of these studies followed the bias correction and statistical downscaling (BCSD) approach described by Salathé et al. (2007), Wood et al. (2004, 2002). The third approach is to utilize regional climate model simulations constrained by GCMs to drive hydrologic models. Significant resources are required to implement this approach, limiting its use. Nonetheless, this approach was the basis for a companion paper by Salathé et al. (2010).

The advantage of the BCSD approach is that it makes direct use of transient climate change scenarios and, therefore, incorporates projected changes in climate variability. There are, however, some key assumptions in the spatial and temporal downscaling that can complicate interpretation of results at sub-monthly (e.g., daily or weekly) time steps. In addition, evaluation of transient scenarios is complicated by the stochastic element of the transient climate variability. Full analysis of this effect requires a large number of ensemble members; however, most GCMs archive only a single transient run, and even for those that archive multiple ensembles, the number is generally quite small. The primary advantage of the delta method approach is that it provides realistic temporal sequencing associated with the historic record, while avoiding bias in the GCM simulations. Another advantage is that climate change impacts may be evaluated in the context of historical events. However, the primary disadvantage is that we do not incorporate projected changes in climate variability by the GCMs into the hydrologic simulations. The delta method approach is arguably more appropriate for this study to evaluate water resource system performance at a sub-monthly timestep in a changing climate, as reported in companion papers by Hamlet et al. (2010) and Vano et al. (2010a, b).

We performed hydrologic simulations to evaluate the impacts of climate change on statewide hydrology in the 2020s, 2040s and 2080s. The delta values represent monthly average changes for each future period over the whole PNW. The PNW is arguably the smallest area that the GCMs are able to resolve and, therefore, potential differences in rates of climate change across Washington State are not incorporated. Each future period represents a 30-year average of projected climate; for instance, the 2020s are represented by the 30-year average climate between 2010 and 2039. Likewise for the 2040s and 2080s, these represent the average climate over 30-year periods 2030–2059 and 2070–2099, respectively. Six composite scenarios were formed following methods outlined by Mote and Salathé (2010). In particular, for each 30-year time period and each month, we computed domain-average precipitation and temperature changes. Unlike Mote and Salathé (2010), we assume equal weighting of each climate change scenario for this study because, as similarly found by Brekke et al. (2004), the weighting of scenarios is largely dependent on the criteria used. In accordance with the delta method approach, we perturbed the entire spatially gridded record of observed historical daily precipitation and temperature (water years 1917–2006) by the projected change for the corresponding month (12 values for each of precipitation and temperature), for each of the three future periods.

In addition to performing hydrology simulations over the PNW using composite scenarios, we also performed simulations using 39 individual scenarios of 2020s climate over focus watersheds of the Yakima River and the Puget Sound for each of the GCMs. The ensemble of simulations allows for better understanding of the range of uncertainty of projections in the focus watersheds.

2.3 Focus watersheds

We evaluated in more detail the impacts of projected future climate change on the hydrology of two key areas: The drainages to the Puget Sound and the Yakima River watershed. These two focus regions are shown in Fig. 1.

The Puget Sound domain is bounded to the east by the Cascades and to the west by the Olympic Mountains, and covers an area of approximately 30,000 km^2. Its elevation ranges from sea level to 4,400 m. Substantial winter snowfall occurs at high elevations, but rarely in the lowlands. Annual precipitation ranges from 600 to over 3,000 mm, depending on elevation, most of which falls from October to March. The watersheds that drain to the Puget Sound are generally characterized as transient. The Puget Sound domain includes more than 69% of the State's population (based on 2000 census). Quantification of the region's future water supply is therefore critical to the region's future growth and ecosystem conservation. We focus here on four Puget Sound watersheds that are managed primarily for water supply: the Cedar River, Green River, South Fork (SF) Tolt River, and Sultan River (Fig. 1). In a companion paper (Vano et al. 2010a), we use the hydrological sequences described herein as input to reservoir simulation models. In this paper, we limit our attention to the hydrological projections.

The Yakima River, which drains east through an arid lowland area, supplies water to over 180,000 irrigated hectares (450,000 acres). Agriculture in the Yakima River watershed has changed over time. Land used to grow annual crops (e.g. wheat) has decreased, while that used to grow perennial crops including apples and grapes has increased. This shift toward perennial crops has increased the dependence of agricultural producers on reliable water supplies (EES, Inc. 2003). Vano et al. (2010b) use the hydrological sequences described herein in conjunction with a reservoir simulation model of the Yakima River watershed to evaluate potential climate change impacts on agricultural production in the basin.

3 Model sensitivities to changes in climate

By the 2040s, future regional temperatures are projected to be out of the range of historic variability (Mote and Salathé 2010). Further, we lack observations to evaluate the sensitivity of hydrologic models to projected changes in climate, which makes evaluation of confidence in predicting impacts difficult. The need for "validation" of hydrological models is widely accepted in the hydrological literature, and it is usually performed by using split sample methods, first to estimate model parameters, and then to evaluate model performance (see e.g. Refsgaard and Storm 1996). However, a similar structure for evaluation of model sensitivities, such as how much runoff will change for a given amount of warming, is often lacking. Dooge (1992) suggested a framework for assessing hydrological sensitivity to changes in precipitation or PET. Precipitation sensitivity can be evaluated on an annual basis from historical observations of runoff or streamflow. Runoff may be used as a surrogate for streamflow in calculation of sensitivity because, on an annual basis, the difference introduced by the time lag of streamflow routing is negligible. Unlike precipitation, PET is commonly computed, rather than observed, and it depends on net radiation, vapor pressure deficit, wind, and land surface properties. Several of these variables are temperature dependent. Furthermore, hydrological sensitivities to temperature are generally much more subtle than to precipitation, and they are difficult to estimate from observations because precipitation effects dominate the results. Therefore, here we focus on sensitivity of runoff to changes in precipitation and temperature independently.

Previous studies show that precipitation sensitivity performed on the same watershed using different hydrologic models can lead to different results. For example, the results from Nash and Gleick (1991) and Schaake (1990) for the Colorado River differ in their precipitation sensitivities by a factor of about two. Sankarasubramanian et al. (2001) suggested a non-parametric, robust, and unbiased estimator (called elasticity) which summarizes sensitivity of streamflow to changes in precipitation, which yields similar results for a wide range of hydrologic model structures. Their estimator of the streamflow sensitivity to precipitation is:

$$e_p = \text{median}\left(\frac{Q_t - \overline{Q}}{P_t - \overline{P}} * \frac{\overline{P}}{\overline{Q}}\right) \tag{1}$$

where Q_t and P_t are annual streamflow and precipitation, respectively, and $\overline{Q}$ and $\overline{P}$ are the long-term mean annual streamflow and precipitation.

A result of the Sankarasubramanian et al. (2001) work was a contour map for the continental USA of (annual) streamflow sensitivities to precipitation. The map shows streamflow sensitivities in the range 1.0–2.0 for much of Washington State. In other words, a given change in precipitation would result in a one- to two-fold increase in streamflow. Using Eq. 1, we evaluated observed and simulated runoff sensitivities to precipitation for six locations within the Yakima watershed and six in the Puget Sound domain. These locations are noted in Fig. 1 (overview map) and are defined in Table 3. Sensitivities for the Yakima River watersheds were calculated using results from the VIC model, while sensitivities for the Puget Sound were calculated using the DHSVM model.

We computed runoff sensitivity to temperature as the percent change in runoff per 1°C of warming, using two methods. The first is a fixed temperature increase, in

Table 3 Summary of analysis locations

Site ID	Description	Basin area (km^2)	USGS ID
Yakima Watershed			
BUMPI	Bumping River near Nile	184	12488000
RIMRO	Tieton River at Tieton Dam near Naches	484	12491500
KACHE	Kachess River near Easton	166	12476000
KEEMA	Yakima River near Martin	142	12474500
CLERO	Cle Elum River near Roslyn	526	12479000
YAPAR	Yakima River near Parker	6,889	12505000
Columbia Watershed			
DALLE	Columbia River at the Dalles	613,827	14105700
Puget Sound			
Cedar E	Cedar River at Renton	469	12119000
Green C	Green River Outlet near Auburn	1,032	NA
Cedar A	Cedar River near Cedar Falls	106	12115000
Green A	Green River above Howard Hanson Dam	573	NA
Sultan A	Sultan River	178	NA
Tolt A	South Fork Tolt River near Index	17	12147600

Sites with USGS ID of “NA” indicate these are not USGS gage locations

which both daily maximum and minimum temperature were increased by 1°C. In the Maurer et al. (2002) formulation of land surface forcing variables which are used by the VIC model, downward solar radiation is indexed to the daily temperature range, hence for the same increase in Tmin and Tmax, downward solar radiation is constant (however, net longwave radiation, as well as vapor pressure deficit, both change). Such a fixed temperature increase was used to develop delta method scenarios in this study.

The second computation also changes the daily average temperature by 1°C, but leaves Tmin unchanged, while increasing Tmax by 2°C. This has the effect of increasing downward solar radiation, but leaving the dew point (which is directly related to the daily minimum temperature in the model) unchanged. Meehl et al. (2007) summarizes projected changes in the global diurnal temperature range (i.e. difference between Tmax and Tmin). Although this range is expected to change over parts of the globe, there is no consensus among GCMs for the direction of change for the PNW. Therefore, we applied the delta method approach using fixed change in Tmax and Tmin.

We analyzed precipitation and temperature sensitivities for six locations in the Yakima River watershed, which correspond to the five basin reservoir locations, in addition to the Yakima River at Parker (USGS ID 12505000), which is a key reference station for water management in the basin. Observed and simulated precipitation sensitivities calculated from the historical record for these sites are in close agreement and are summarized in Table 4. They range from 1.08 to 1.42 in the Yakima watershed. A 10% increase in precipitation causes an increase in runoff by a factor of 1.59 for the entire basin (at Parker) to 1.87 for Bumping Lake, which has a small contributing area (184 km^2) and is at a relatively high elevation (1,030 m). An average daily temperature increase of 1°C, applied by increasing both minimum and maximum temperature (downward solar radiation unchanged), reduces basin runoff by approximately 2.45 (Rimrock) to 5.77% (Bumping Lake) (refer to Table 4, Temperature Sensitivity a). Alternatively, the same average daily

Table 4 Summary of precipitation and temperature sensitivities at analysis locations

Site	Observed (and simulated) precipitation sensitivity	Precipitation sensitivity (10% increase)	Temperature sensitivity (a), %/°C	Temperature sensitivity (b), %/°C
Yakima Watershed				
BUMPI	1.42 (1.12)	1.87	−5.77	−9.81
RIMRO	1.37 (1.08)	1.65	−2.45	−6.26
KACHE	1.16 (1.23)	1.67	−3.70	−6.36
KEEMA	1.15 (1.19)	1.78	−5.19	−7.56
CLERO	1.12 (1.13)	1.61	−4.01	−6.73
YAPAR	1.32 (1.32)	1.59	−2.84	−5.15
Puget Sound				
Cedar E	1.38 (1.22)	1.36	−1.11	−2.99
Green C	1.33 (1.43)	1.63	−2.33	−5.57
Cedar A	1.08 (1.17)	1.28	−1.05	−2.77
Green A	1.42 (1.37)	1.61	−2.42	−5.64
Sultan A	1.06 (1.12)	1.17	−0.69	−1.69
Tolt A	1.12 (1.00)	1.20	−0.66	−1.50

Precipitation sensitivity is defined as the ratio of the fractional change in runoff to the fractional change in precipitation. Temperature sensitivities are defined as the percent change in runoff per 1°C of warming. Temperature sensitivity (a) considers increased daily minimum and maximum temperature, while temperature sensitivity (b) considers increased daily maximum temperature

increase, by altering maximum temperature only (constant dew point), reduces runoff by 5.15% (Parker) to 9.81% (Bumping Lake) (refer to Table 4, Temperature Sensitivity b).

In the Puget Sound, we analyzed six catchments including the Cedar River at Renton, (Cedar E), the Cedar River near Cedar Falls (Cedar A), Green River near Auburn (Green C), the Green River above Howard Hanson Dam (Green A), the Sultan River (Sultan A) and the South Fork Tolt River near Index (Tolt A; see Fig. 1 for locations). These points are generally located near water supply reservoirs. Precipitation sensitivity for observed and simulated historical periods at the six sites are in agreement (see Table 4) with values ranging from 1.0–1.4. An increase in precipitation of 10% for the same simulated watersheds (with temperature remaining unchanged) causes an increase in runoff by a factor of 1.17 to 1.63 in the Puget Sound. An average temperature increase of 1°C, by increasing both maximum and minimum temperature by 1°C (see Table 4, Temperature Sensitivity a), results in approximately a 0.7–2.4% decrease in streamflow in the Puget Sound watersheds. The same average increase in daily temperature applied by increasing the maximum temperature by 2°C and leaving the minimum temperature unchanged (see Table 4, temperature sensitivity b) results in decreases in runoff by 1.5–5.6%.

Runoff sensitivity to temperature change is expected to be higher when only Tmax is increased as compared with increasing both the Tmax and Tmin because when both are increased by a fixed amount, the downward solar radiation remains constant. As a result, the change in net radiation is generally smaller than when the minimum temperature is left unchanged. On the other hand, many analyses of trends in the daily temperature range (e.g. Easterling et al. 1997) indicate decreases (mostly resulting from more rapid upward trends in daily minimum temperatures than in the daily maxima) and for this reason, use of the delta method may somewhat overestimate the effects of climate warming on snowpack reduction and evapotranspiration increases.

The basis for different precipitation and temperature sensitivities across sites is less clear. Sensitivities are generally higher for Yakima watershed sites than for Puget Sound sites, but it is not entirely clear whether these differences are related to watershed characteristics or to potentially different sensitivities of the two hydrologic models. Comparisons of some aspects of VIC and DHSVM relative sensitivities (to land cover, rather than climate change) have been made (e.g. VanShaar et al. 2002), however the relative climatic sensitivities have not, warranting future study. The precipitation and temperature sensitivities calculated above are based on annual changes. Runoff responses will vary depending on the seasonality of change. Nonetheless, understanding of hydrologic sensitivities to temperature and precipitation on an annual basis does provide some useful context for recognizing the nature of these sensitivities to climate change, which is emerging from a rapidly expanding literature on the topic.

4 Results and discussion

Projections of 21st century climate of the PNW summarized in Mote and Salathé (2010) indicate that temperatures will increase an average of 0.3°C (0.5°F) per decade. Changes in annual mean precipitation are projected to be modest, with a projected increase of 0.2–1.9% by the 2020s and 2.1–2.2% by the 2040s. However, the range of projected precipitation shows a decrease of almost 10% to an increase of almost 21% by the 2080s, underscoring the uncertainty in projections of future precipitation. Projected temperature increases, along with changes in seasonal precipitation have important implications for hydrologic variables across Washington. In this section we summarize impacts of projected changes in climate on a state level, and then provide a more focused evaluation of watersheds within the Puget Sound and the Yakima River watershed. Projected changes reported in this section are comparisons with the mean over water years 1917–2006.

4.1 Statewide climate change impacts

4.1.1 Implications of changes in April 1 snow water equivalent

Many past studies demonstrate that changes in snowpack are a primary impact pathway associated with regional warming in the PNW (Lettenmaier et al. 1999; Hamlet and Lettenmaier 1999; Snover et al. 2003). Changes in snowpack are affected by both precipitation and temperature, although in the twentieth century, temperature has been the primary driver (Mote et al. 2005; Hamlet et al. 2005; Mote 2006; Mote and Salathé 2010), particularly in relatively warm areas such as the Cascades. SWE on April 1 is an important metric for evaluating snowpack changes because in the PNW, the water stored in the snowpack on April 1 is strongly correlated with summer water supply.

Figure 5 shows projected changes in April 1 SWE for the 2020s, 2040s, and 2080s for the composite A1B and B1 climate conditions, as simulated using the VIC model. Results from these hydrologic simulations are consistent with previous studies, such as the climate impacts study conducted for King County, Washington,

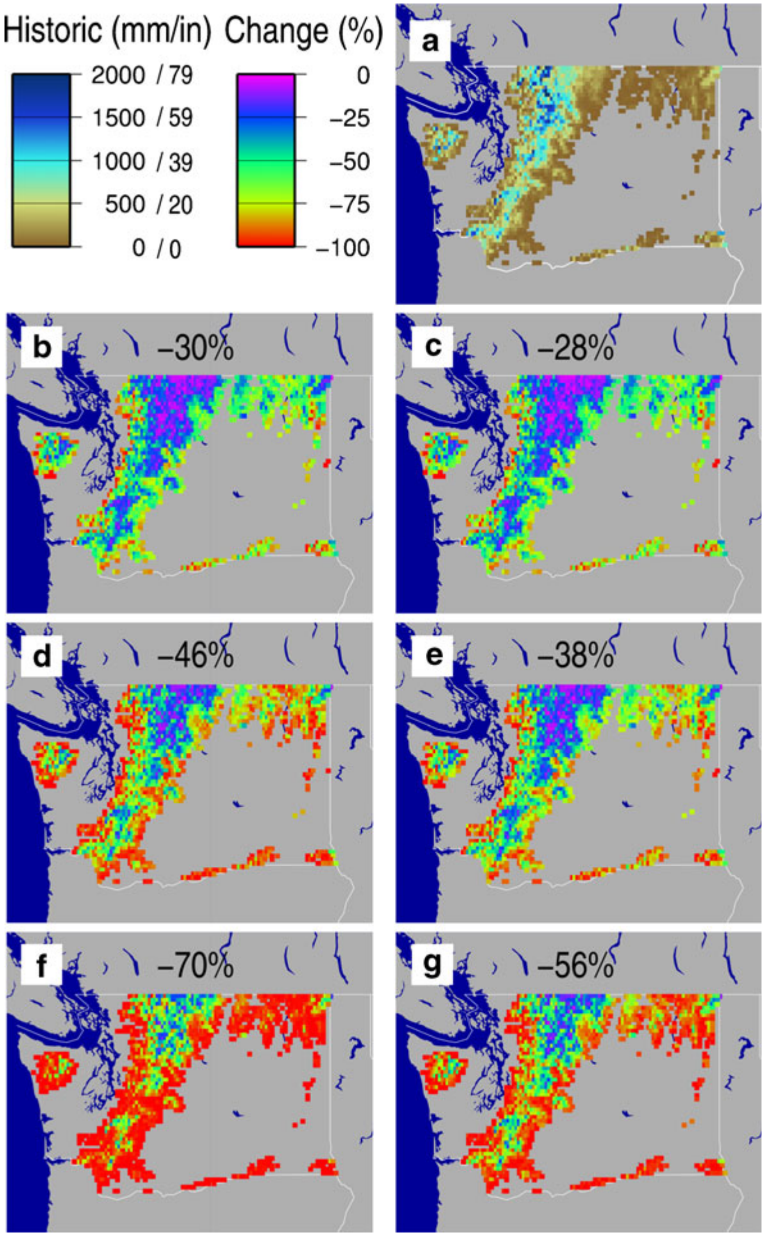

Fig. 5 Summary of projected percent change in April 1 SWE as simulated by the VIC model. **a** Historical April 1 SWE (mean over water years 1917–2006). **b**, **c** Projected change in April 1 SWE for the 2020s (A1B and B1 SRES scenarios, respectively). **d**, **e** Projected change in April 1 SWE for the 2040s (A1B and B1 SRES scenarios, respectively). **f**, **g** Projected change in April 1 SWE for the 2080s (A1B and B1 SRES scenarios, respectively). Percent change values represent spatially averaged April 1 SWE across Washington State with respect to the historical period

Table 5 Projected changes (%) in April 1 snow water equivalent (SWE) according to elevation using delta method composite climate change scenarios (30-year average changes not weighted) for the 2020s, 2040s, and 2080s

Elevation range	Historical SWE (mm)	% Change in April 1 SWE					
		2020s (2010–2039)		2040s (2030–2059)		2080s (2070–2099)	
		A1B	B1	A1B	B1	A1B	B1
< 1, 000 m (<3,280 ft)	21	−40%	−38%	−58%	−49%	−80%	−68%
1,000–1,999 m (3,280 ft–6,558 ft)	365	−27%	−25%	−43%	−35%	−67%	−53%
≥2,000 m (≥6,558 ft)	931	−17%	−15%	−30%	−23%	−55%	−39%
Overall	76	−30%	−28%	−46%	−38%	−70%	−56%

which projected a decrease in snowpack over the twenty-first century (Casola et al. 2005). Generally, results using the B1 emissions scenario project less significant impacts than those using the A1B scenario. Based on composite scenarios for the B1 and A1B scenarios respectively, April 1 SWE is projected to decrease by 28 to 30% across the State by the 2020s, 38 to 46% by the 2040s and 56 to 70% by the 2080s.

Changes in SWE vary by elevation, as Fig. 5 suggests. We summarized these changes over three bands of elevation, specifically elevations below 1,000 meters, between 1,000 and 2,000 meters, and above 2,000 meters (see Table 5). The results show that the lowest of these elevation bands will experience the largest decreases in snowpack, with reductions for B1 and A1B emissions scenarios, respectively, of 38 to 40% by the 2020s to 68 to 80% by the 2080s. The reduction of snowpack in the highest elevation bands is projected to be less significant.

Projected changes in snowpack are directly correlated with temperature. The greatest sensitivity of snowpack to warming is at elevations characterized by winter

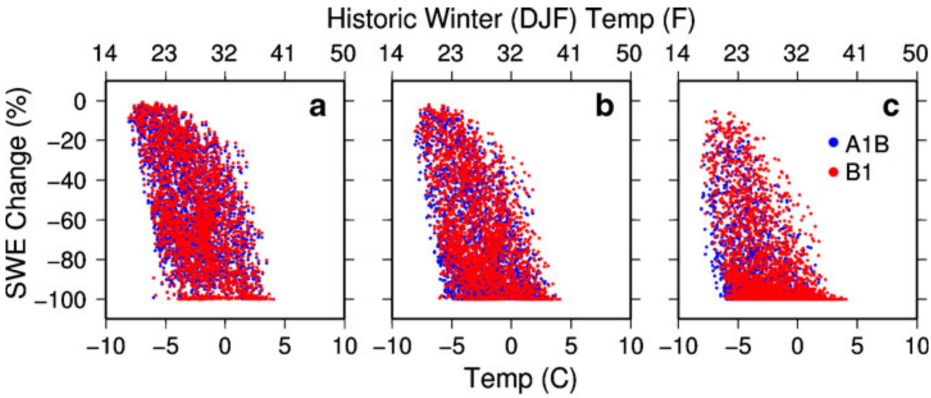

Fig. 6 Projected change in April 1 snow water equivalent (SWE) for the 2020s (**a**), 2040s (**b**), and 2080s (**c**) plotted against mean historical winter temperature (water years 1917–2006). Individual points represent individual VIC model grid cells. Percent changes in April 1 SWE values were derived using a delta method approach, where historical temperature and precipitation were perturbed by the projected average monthly changes for the 2020s (average change from 2010–2039), 2040s (average change from 2030–2059), and 2080s (average change from 2070–2099) and compared with the long-term historical mean for 1917–2006 (water year). Cells with historically trace amounts of April 1 SWE (less than 1 mm) are not included in the plot

temperatures near freezing. Locations with a warmer mean historical winter temperature (defined as December through February) are projected to experience the greatest reduction of snowpack, while locations with cooler winter temperatures are projected to experience more modest reductions (Fig. 6). Projections using the A1B emissions scenario generally show greater reductions in snowpack than those using the B1 scenario, especially for the 2080s simulations.

4.1.2 Implications of changes in July 1 soil moisture

Vegetation and dry land agriculture rely heavily on soil moisture, in addition to precipitation, particularly in the arid region of the State (east of the Cascades in the Columbia River basin) where summer precipitation is low. Soil moisture in snow dominated watersheds (like the Columbia River basin overall) tends to peak in spring or early summer, in response to melting mountain snowpack. In the summer, lower precipitation (along with clearer and longer days) and increased vegetative activity cause depletion of soil moisture, resulting in minimum soil moisture values in September.

Simulated soil moisture by hydrologic models is strongly determined by model assumptions (Liang et al. 1998), but when expressed as percentiles, many of these differences are removed (Wang et al. 2009). For this reason, we present projected soil moisture changes across the State as percentiles of simulated historic mean soil moisture (water years 1917–2006), where a projected decrease in soil moisture is represented by percentiles less than 50 and a projected increase is represented by percentiles greater than 50. Specifically, we summarize projections of July 1 soil moisture from the VIC model, since this is the typical period of peak soil moisture which is critical for water supply in the state's arid regions.

Projections of July 1 total soil moisture change for the composite A1B and B1 scenarios are modest, but generally show decreases across the State. Projected decreases are greater for A1B scenario simulations compared with B1 simulations. For the three future periods, soil moisture is projected to be in the 38th to 43rd percentile (A1B and B1, respectively) by the 2020s, 35th to 40th percentile by the 2040s, and 32nd to 35th percentile by the 2080s, with 50% being equal to mean historical values. However, projected soil moisture changes vary on either side of the Cascade Mountains. In the mountains and coastal drainages west of the Cascades, a warming climate tends to enhance soil drying in the summer and, in combination with reduced winter snowpack and earlier snowmelt, causes decreases in summer soil moisture (Fig. 7). East of the Cascades, summer soil moisture is primarily driven by recharge of snowmelt water into the deep soil layers. Increased snowpack at the highest elevations in some parts of the Cascades (tied to projected increases in winter precipitation) and subsequently increased snowmelt, are likely to cause greater overall infiltration. Similar trends east and west of the Cascades were found in the study of PNW regional climate change impacts (Casola et al. 2005).

4.1.3 Implications of changes in mean annual runoff and streamflow

As noted by Mote and Salathé (2010), there is a wide range in projections of future precipitation across GCMs and SRES emissions scenarios. Across the 39 scenarios considered in this study (20 GCMs and two SRES emissions scenarios for all but one GCM), projected annual precipitation changes over the PNW range from −9%

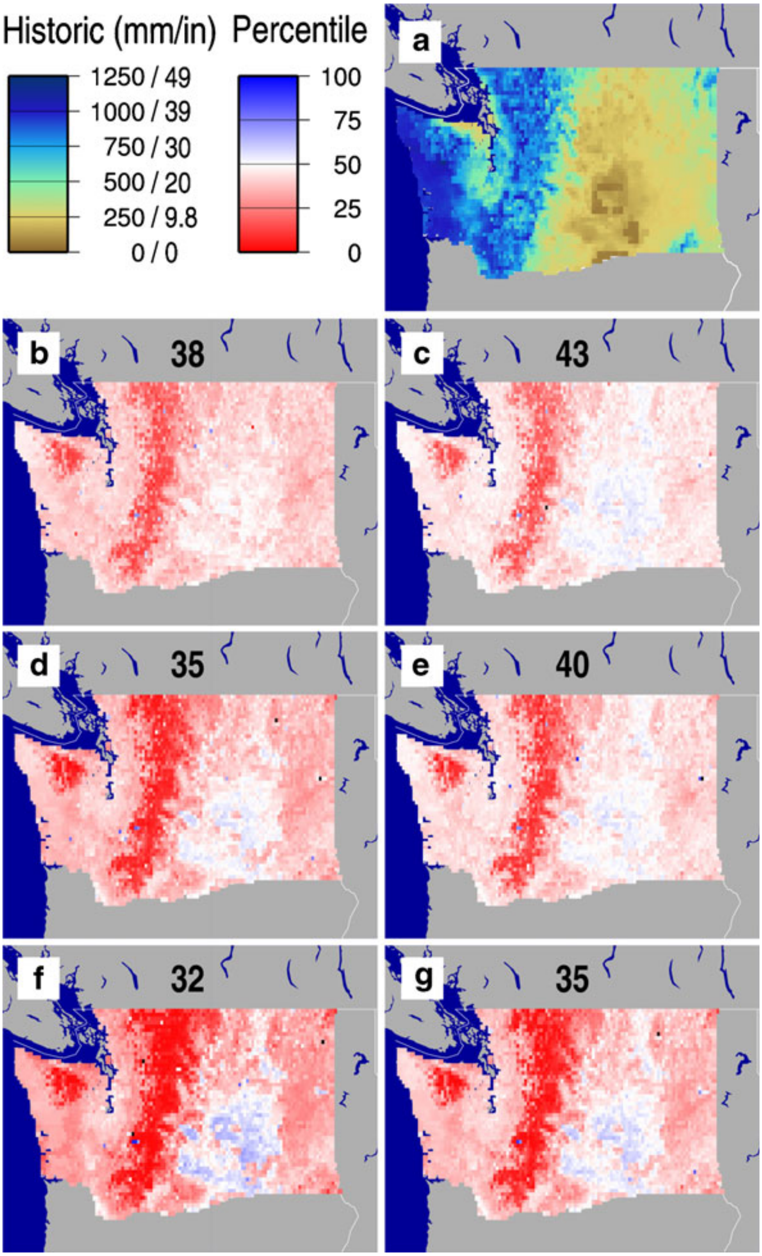

Fig. 7 Summary of projected change in July 1 soil moisture as a percentile of simulated historical mean from water year 1917–2006 (using the VIC model). **a** Historical July 1 soil moisture. **b**, **c** Projected change in July 1 soil moisture for the 2020s (A1B and B1 SRES scenarios, respectively). **d**, **e** Projected change in July 1 soil moisture for the 2040s (A1B and B1 SRES scenarios, respectively). **f**, **g** Projected change in July 1 soil moisture for the 2080s (A1B and B1 SRES scenarios, respectively). Percentiles less than 50 represent a decrease in soil moisture, while percentiles greater than 50 show an increase in soil moisture. Reported values represent spatially averaged percentiles across Washington State

Table 6 Summary of composite changes in annual precipitation and runoff across Washington using composite delta method scenarios (30-year average changes not weighted) for the 2020s, 2040s, and 2080s for SRES A1B and B1 global emissions scenarios

	2020s (2010–2039)		2040s (2030–2059)		2080s (2070–2099)	
	A1B	B1	A1B	B1	A1B	B1
Change in temperature	+1.18°C	+1.08°C	+2.05°C	+1.57°C	+3.52°C	+2.49°C
% Change in precipitation	+0.22%	+1.86%	+2.08%	+2.20%	+4.92%	+3.40%
% Change in runoff	−0.1%	+2.2%	+2.5%	+2.1%	+6.2%	+4.0%

to +12% for the 2020s, −11% to +12% for the 2040s, and −10% to +21% for the 2080s, with modest increases projected for the composite scenarios for A1B and B1 (Table 6). Although projected increases of annual precipitation are modest, projections of seasonal precipitation change indicate increased winter precipitation and decreased summer precipitation (Tables 7 and 8). With most of the annual precipitation falling between October and March (Hamlet and Lettenmaier 1999), cool season precipitation is the primary driver of hydrologic processes in Washington and the PNW. Projections of cool season precipitation for the composite B1 and A1B scenarios, respectively, range from +2.3% to +3.3% for the 2020s, +3.9% to 5.4% for the 2040s, and +6.4% to +9.6% for the 2080s (Table 7). Table 6 summarizes the composite projected changes in annual precipitation and corresponding state-wide changes in runoff simulated by the VIC model. The importance of cool season precipitation to the State's runoff is evident: even with increased temperatures and modest, as opposed to significant, annual precipitation increases, runoff increases in all cases except in the case of the 2020s for emissions scenario A1B where we see a slight decrease in annual runoff. This contrasts with results for precipitation and temperature sensitivities (Table 4) to the extent that on an annual basis, the modest precipitation changes coupled with temperature increases should have led to runoff reductions. The reason this is not the case is that in the Table 4 experiments, precipitation changes are uniform over the year, whereas in the GCM output (at least for the composites), cool season precipitation, a more efficient producer of runoff than summer precipitation due to higher soil moisture storage and lower vegetative water demand, increases while summer precipitation decreases.

These results differ from the projected changes in runoff presented by Milly et al. (2005), who summarized average changes in runoff over Water Resources Regions across the continental U.S. and Alaska, defined by the US Water Resources Council for the period 2041–2060, relative to 1901–1970. Their projections are based on output from 12 IPCC AR4 GCMs and the A1B SRES scenario, and showed slight

Table 7 Summary of composite changes in cool season (October through March) precipitation and runoff across Washington using delta method composite climate change scenarios (30-year average changes not weighted) for the 2020s, 2040s, and 2080s for SRES A1B and B1 global emissions scenarios

	2020s (2010–2039)		2040s (2030–2059)		2080s (2070–2099)	
	A1B	B1	A1B	B1	A1B	B1
Change in temperature	+1.05°C	+1.01°C	+1.83°C	+1.42°C	+3.24°C	+2.33°C
% Change in precipitation	+2.3%	+3.3%	+5.4%	+3.9%	+9.6%	+6.4%
% Change in runoff	+10.7%	+12.4%	+20.2%	+15.9%	+34.0%	+25.2%

Table 8 Summary of composite changes in warm season (April through September) precipitation and runoff across Washington using delta method composite climate change scenarios (30-year average changes not weighted) for the 2020s, 2040s, and 2080s for SRES A1B and B1 global emissions scenarios

	2020s (2010–2039)		2040s (2030–2059)		2080s (2070–2099)	
	A1B	B1	A1B	B1	A1B	B1
Change in temperature	+1.31°C	+1.16°C	+2.26°C	+1.71°C	+3.79°	+2.66°C
% Change in precipitation	−4.2%	−0.9%	−5.0%	−1.3%	−4.7%	−2.2%
% Change in runoff	−19.8%	−16.4%	−29.6%	−23.0%	44.2%	−34.4%

decreases in runoff of 2–5% across the PNW. The 12 GCMs they used are a subset of the 21 (IPCC AR4) models used in this study. Milly et al. (2005) average over 24 ensembles from the 12 models (i.e. for some GCMs, multiple experiments were conducted on the same model); however, the number of ensembles was not the same for each GCM, which effectively weights some models more heavily than others. In addition, Milly et al. (2005) used land surface schemes embedded in the GCMs, which are at coarser resolution than the VIC model and do not resolve the topography of the PNW.

Projections of streamflow differ from those of runoff because runoff is a spatial quantity that is an integral part of the water balance at each hydrologic model grid cell and does not incorporate the time lag effects that contribute to streamflow. Runoff is useful for evaluating projected basin-wide changes as a direct effect of precipitation and snow storage or melt. Streamflow, however, is the culmination of hydrologic processes evaluated at a given location over time. Figure 8 shows projected mean hydrographs for the example rain-dominant, transient, and snow-dominant watersheds in Fig. 4. In the Chehalis River, which drains a rain-dominant watershed, projected changes to the mean hydrograph are minimal. Changes in the mean hydrograph at The Dalles, the outlet of a snowmelt dominant watershed, are more apparent, including reduced peak flow in the late spring and early summer and increased cool season flow in connection with reduced snowpack. Changes in the Yakima watershed, a transient rain–snow watershed, are significant, indicating a shift to a characteristic rain-dominant watershed by the 2080s. Vano et al. (2010b) describes the implications of this change on water management in the basin.

4.2 Hydrologic case studies

We evaluated impacts of climate change on three focus regions, namely the Columbia River watershed, the Puget Sound, and the Yakima River watershed. Because the Columbia River watershed covers approximately two thirds of Washington State, discussion of impacts in this region is incorporated into the discussion of statewide impacts above. The other two case study domains, select watersheds draining to the Puget Sound and Yakima River watershed, are discussed here. They are both transient regions, meaning they are highly sensitive to climate change; however, they differ with respect to their climatic regime—precipitation is generally much higher in the Puget Sound than in the Yakima, particularly its lower reaches. As noted in Section 2.2, we used the high resolution DHSVM hydrologic model in the relatively small Puget Sound watersheds, and we used the VIC model in the Yakima.

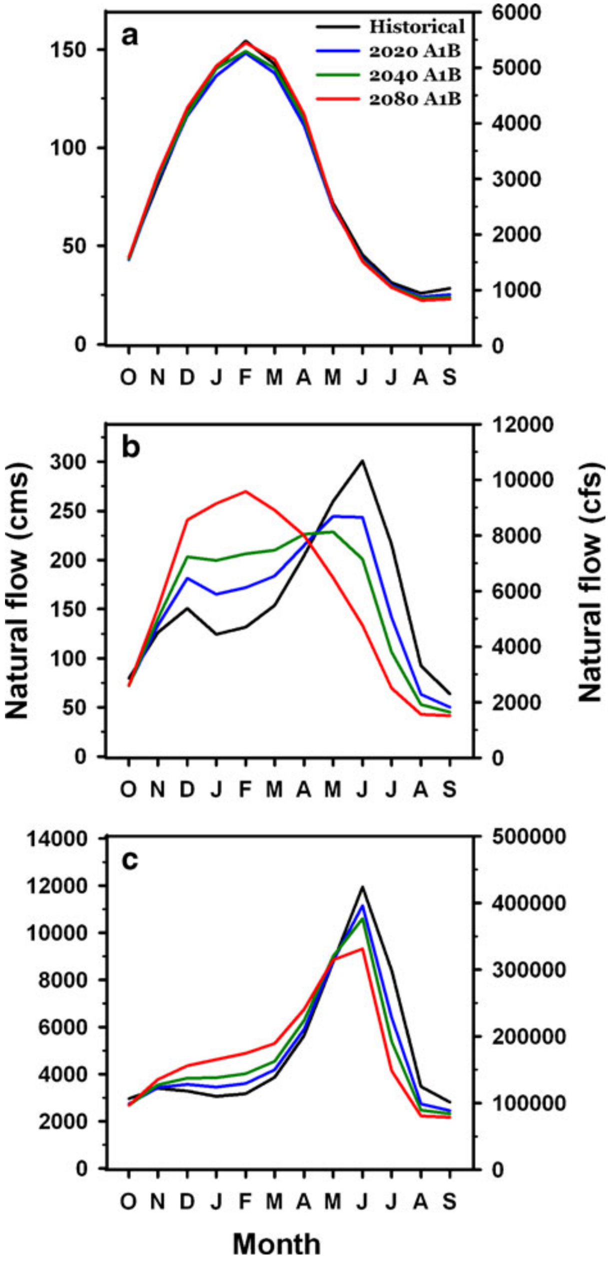

Fig. 8 Projected average monthly streamflow for three representative watershed types in Washington: **a** rain dominant (Chehalis River at Porter), **b** transient rain–snow (Yakima River at Parker), and **c** snowmelt dominant (Columbia River at The Dalles). Hydrographs are monthly averages of simulated daily streamflow by the VIC model for water years 1917–2006) and three future periods (2020s, 2040s, and 2080s) using the A1B SRES scenario

4.2.1 Implications of climate change on Puget Sound catchments

We examined SWE predictions in the headwaters of the Cedar, Sultan, Tolt, and Green River. Figures 9 and 10 show simulated historical April 1 SWE and predicted change of SWE in the 2020s, 2040s and 2080s for A1B and B1 SRES scenarios. In both Figs. 9 and 10, the top panel shows mean historical SWE on April 1, while the

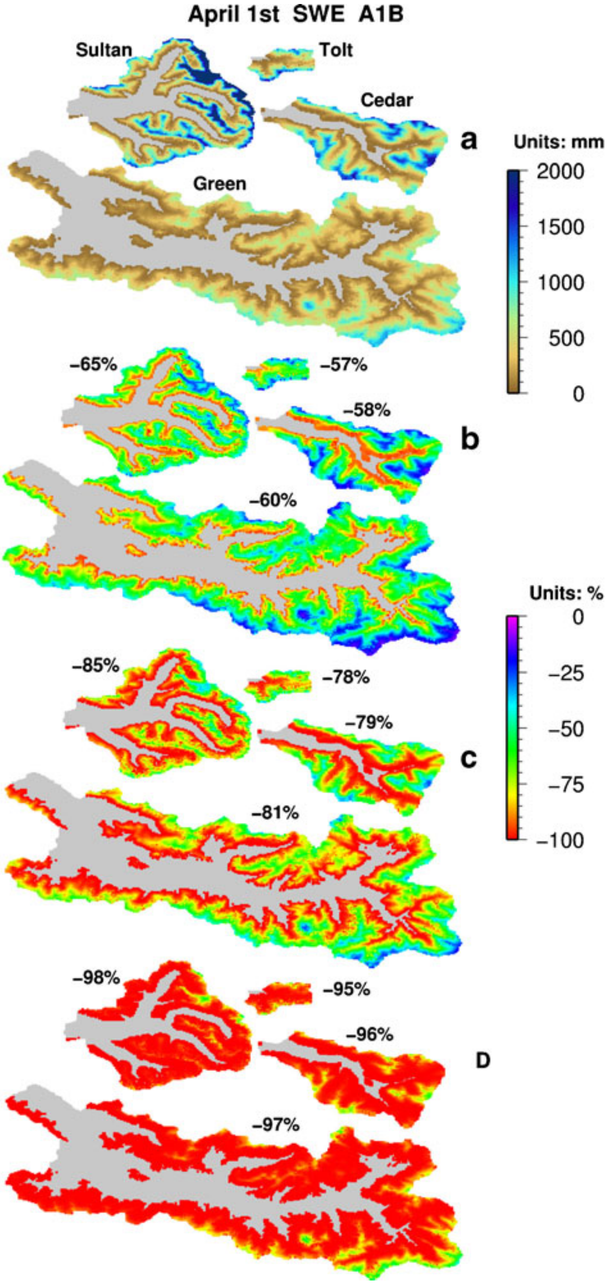

Fig. 9 Projected changes in snow water equivalent (SWE) in the headwaters of four Puget Sound watersheds for the 2020s (**b**), 2040s (**c**), and 2080s (**d**) compared with simulated mean historical (water years 1917–2006) April 1 SWE (**a**) as simulated by the DHSVM for the A1B SRES scenario. Watershed locations are illustrated in Fig. 1

bottom three panels show projected changes in percent. For each time period, the watershed at top left illustrates the upper part of the Sultan River watershed, the top right shows the upper Tolt River watershed, the middle right shows the upper Cedar River watershed, and the lower shows the upper Green River watershed.

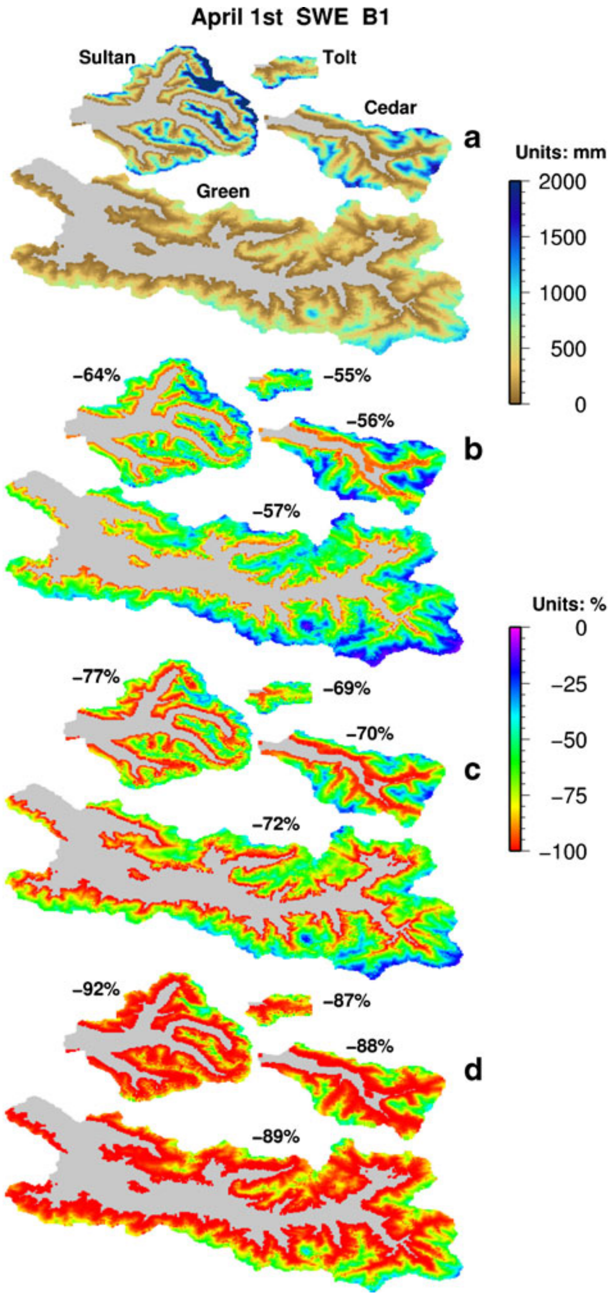

Fig. 10 Projected changes in snow water equivalent (SWE) in the headwaters of four Puget Sound watersheds for the 2020s (**b**), 2040s (**c**), and 2080s (**d**) compared with simulated mean historical (water years 1917–2006) April 1 SWE (**a**) as simulated by the DHSVM for the B1 SRES scenario. Watershed locations are illustrated in Fig. 1

In the 2020s, 2040s and 2080s, the largest decrease in SWE occurs in the watershed valleys as temperature rises. Upper Cedar and Green watersheds have approximately 90% reductions in SWE in the valleys starting from the 2020s, while the Sultan and Tolt watersheds, which are located in higher elevations, have smaller reductions in the 2020s. SWE decreases more substantially in the upper parts of all four basins in the 2040s, and by the 2080s, SWE is projected to disappear. Generally, simulations using the A1B SRES scenario show greater reductions in SWE (Fig. 9) than those using B1 (Fig. 10).

Projected weekly time series of domain-averaged SWE in the four Puget Sound watersheds from the six composite scenarios described earlier for the 2020s, 2040s, and 2080s, as well as from all 39 ensemble scenarios for the 2020s, are summarized in Fig. 11. We summarize the ensemble projections through use of a gray swath which spans the range of results from the 39 ensembles. Weekly values are summarized according to water year, October to September. The figure shows reduction of SWE throughout the winter months, compared to historical simulations. Peak SWE is projected to shift in all watersheds from near week 26 (late March), which is the average historical peak, to near week 23 (early March) by the 2020s and 2040s to near week 20 (mid-February) by the 2080s.

Simulated streamflow at the reservoirs in the four watersheds shows a consistent shift in the hydrograph toward higher runoff in cool season and lower runoff in warm season (Fig. 12). The winter peaks become higher but summer peaks become lower in the 2020s, 2040s and 2080s compared to the historical simulation. Into the future, the double-peak hydrograph transforms into a single-peak hydrograph associated with increasingly rain-dominant behavior. The streamflow timing shift is mainly due to the less frequent snow occurrence, and faster and early snow melt in these historically snow-rain mixed watersheds.

To assess the extent climate change might impact the timing of flow, and thus annual reservoir storage, we compared the time of year at which half of the annual (water year) flow has passed (centroid of timing, see Stewart et al. 2005). The centroid of timing (CT) values were computed from the 1917–2006 (water year) weekly average flows. The seasonal shift is visible in the CT values (Table 9), which for the A1B emissions scenario and 2020s are about 2 weeks earlier for inflows into the Howard Hanson Reservoir on the Green River, 5 weeks earlier for Chester Morse Reservoir inflows on the Cedar River, and 3 weeks earlier for Spada Lake Reservoir on the Sultan River for the 2020s period. CT changes are smaller for B1 emissions scenarios. Given the small size (relative to mean annual inflow) of all three water supply systems, these shifts suggest that there will be increasing challenges in meeting water management objectives (Vano et al. 2010a).

4.2.2 Implications of climate change on the Yakima watershed

Projections of change in April 1 SWE over the Yakima watershed are summarized in Fig. 13 and indicate that for A1B and B1 emissions scenarios, respectively, SWE will decrease by 35% to 37% by the 2020s, 47% to 57% by the 2040s and 68% to 82% by the 2080s. Changes in snowpack projected for the Yakima watershed are higher than projected average changes over the State as a whole (Fig. 5). Weekly SWE was calculated using results from the VIC model and are summarized in the bottom panel of Fig. 11. The bottom panel of Fig. 11 shows historical and projected weekly SWE for the entire watershed. The peak weekly SWE historically occurs near week 24 (mid-March). Projections of weekly SWE for the 2020s indicate that SWE will be reduced by an average of 39% to 41% according to A1B and B1 scenarios, respectively. The peak week is projected to shift earlier to near week 23 (early to mid-March). By the 2040s, SWE will be reduced by 50% to 58% (with a peak projected to occur near

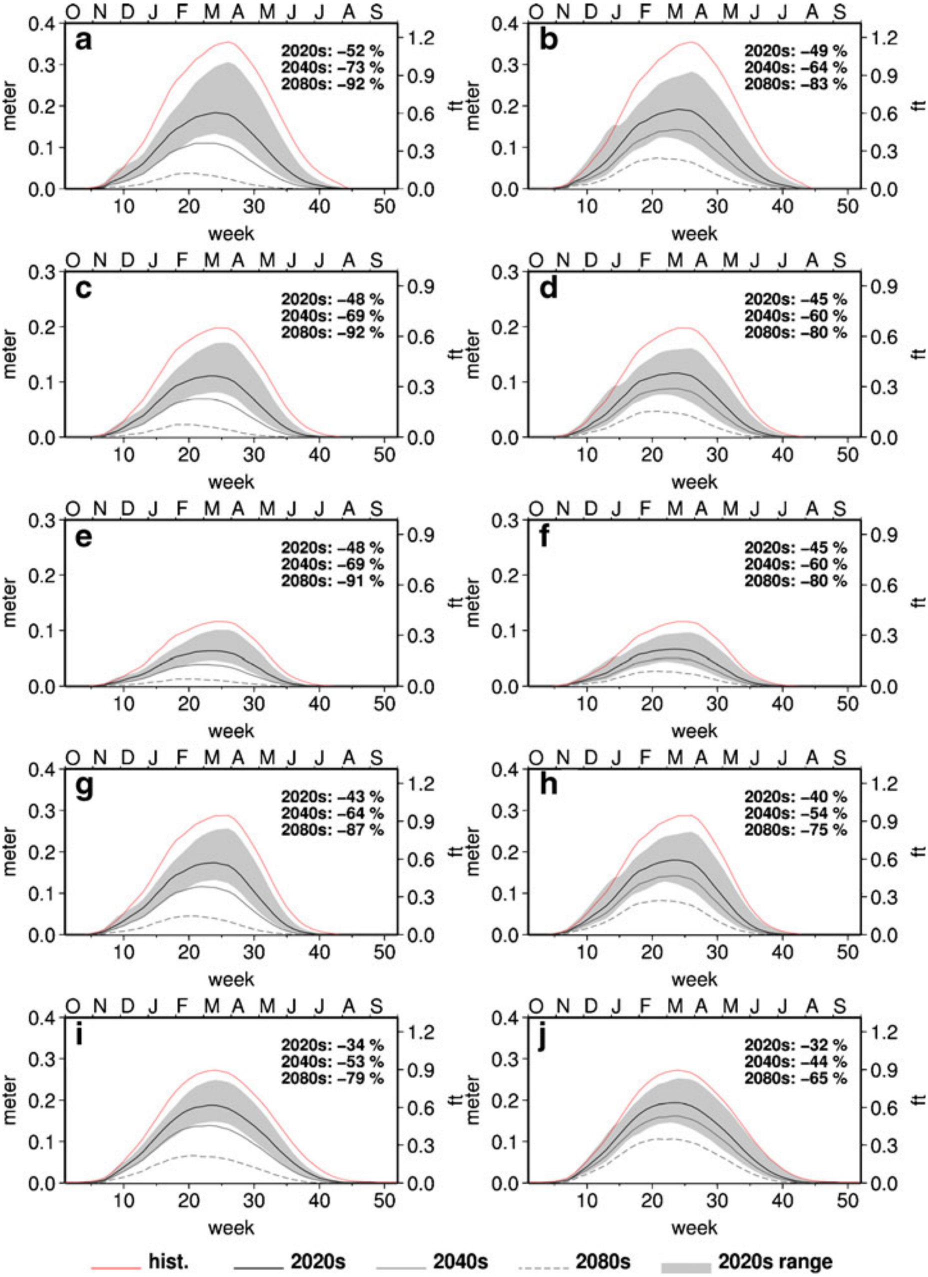

Fig. 11 Projected changes in weekly (within the water year; week 1 begins October 1) snow water equivalent (SWE) for the 2020s, 2040s, and 2080s. Results in the top four pairs of panels are based on DHSVM simulations, while the bottom pair of panels is based on VIC model simulations. Units in meters and feet are provided. **a**, **b** Tolt watershed results for the A1B and B1 scenarios, respectively. **c**, **d** Cedar watershed results (A1B and B1). **e**, **f** Green watershed results (A1B and B1). **g**, **h** Snohomish watershed results (A1B and B1). **i**, **j** Yakima watershed results (A1B and B1)

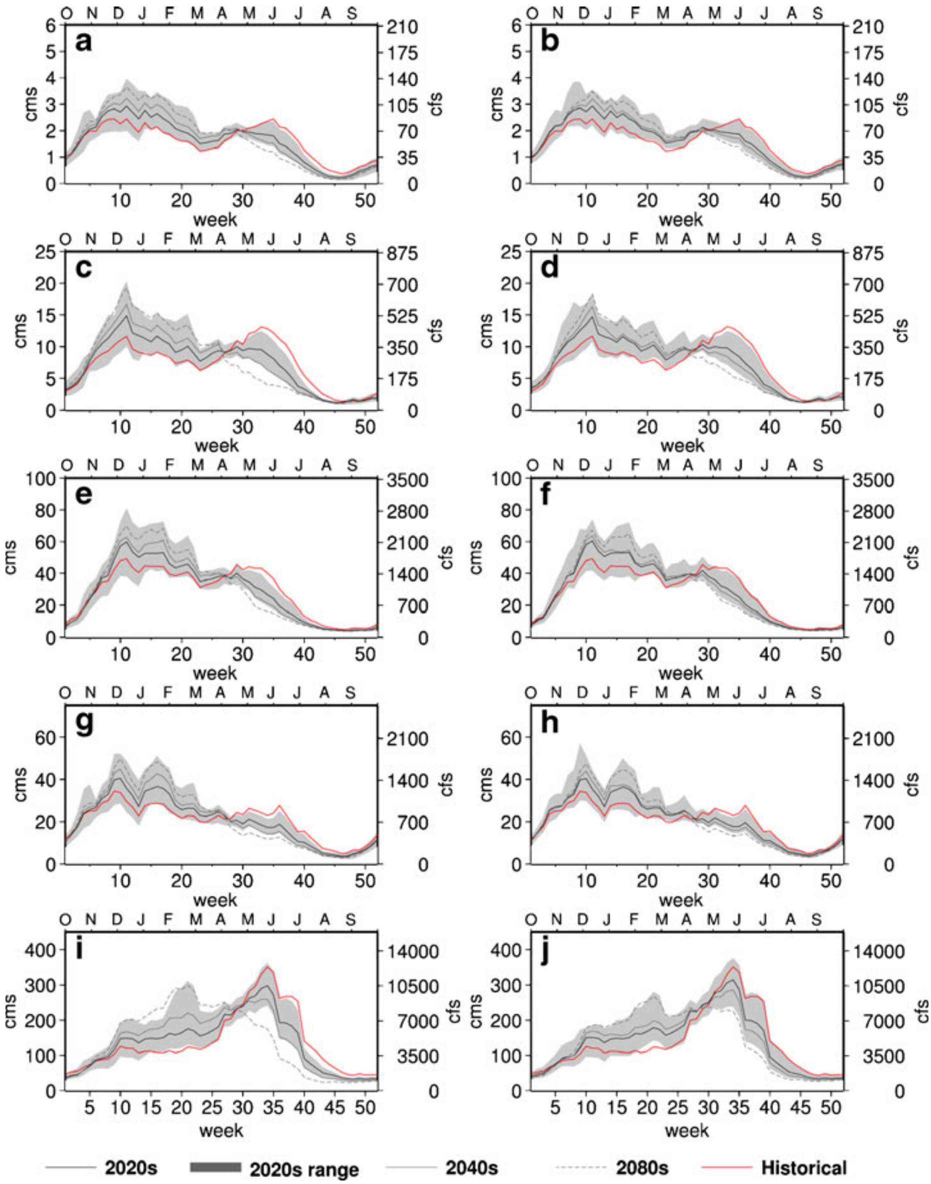

Fig. 12 Projected changes in weekly streamflow for the 2020s, 2040s, and 2080s (A1B and B1 SRES scenarios) compared with weekly mean simulated historical streamflow for water years 1917–2006. Results in the top four pairs of panels are based on DHSVM simulations, while the bottom pair of panels is based on VIC model simulations. Units in cubic meters per second and cubic feet per second are provided. **a**, **b** Tolt watershed results for the A1B and B1 scenarios, respectively. **c**, **d** represent Cedar watershed results (A1B and B1). **e**, **f** Green watershed results (A1B and B1). **g**, **h** Snohomish watershed results (A1B and B1). **i**, **j** Yakima watershed results (A1B and B1)

week 22, or early March), and by 67% to 80% by the 2080s (with a peak projected to occur near week 20, or mid-February).

We also summarized projections of weekly streamflow in the bottom panel of Fig. 12 for the same suite of scenarios evaluated with respect to SWE. Peak streamflow historically occurs near week 34 (mid-May) in the Yakima River at the USGS gage at Parker. The suite of projections for the 2020s indicate that the peak streamflow will not shift significantly; however, increased streamflow in winter is expected. By the 2040s, the spring peak streamflow is projected to shift earlier near week 30 (mid- to late April) and a significant second peak flow is projected in the winter, which is characteristic of historically lower elevation transient watersheds. By the 2080s, a significant shift in the hydrologic characteristics of the watershed are projected, as the spring peak is lost and peak streamflow is projected to occur in the winter near week 20 (mid-February) which is more characteristic of rain dominant watersheds. Thus warming through the 21st century will result in increasingly rain-dominant behavior in the Yakima watershed.

Similar to our analysis for the Puget Sound watersheds, we evaluated the shift in the CT of flow. CT values were computed from the 1917–2006 (water year) weekly average flows for the unregulated flow of the Yakima River at Parker, which provides a representation of naturalized flow throughout the basin. Historically, the CT occurs in mid-April (week 30). In the 2020s scenarios, the CTA seasonal shift is visible in the CT values, which for the A1B emissions scenario and 2020s is about 3 weeks earlier for both A1B and B1 scenarios. In the 2040s and 2080s for the A1B scenarios, flows shift by 6 and 9 weeks respectively. For the B1 scenarios, these shifts are 4 weeks earlier for the 2040s and 7 weeks for the 2080s. These results are summarized in Table 9. These hydrologic changes will have important implications for irrigated agriculture in Washington State (Vano et al. 2010b).

Table 9 Centroids of streamflow timing based on weekly means for the historical period (water year 1917–2006), 2020s, 2040s and 2080s. The centroid is calculated as the time of year at which half of the annual (water year) flow has passed

		Puget Sound				Yakima Watershed
		Sultan A	Cedar A	Tolt A	Green A	YAPAR
	Hist	21	24	22	21	30
AIB scenarios	Min 2020s	17	17	17	17	25
	Avg 2020s	18	19	18	19	27
	Max 2020s	20	21	20	20	29
	2040s	17	18	17	18	24
	2080s	16	16	16	17	21
B1 scenarios	Min 2020s	16	18	17	18	25
	Avg 2020s	18	20	19	19	27
	Max 2020s	20	22	20	20	29
	2040s	17	19	18	18	26
	2080s	16	17	17	17	23

*Values indicate week numbers within the water year, where:
Week 15 is Jan 7
Week 20 is Feb 11
Week 25 is Mar 18
Week 30 is Apr 22

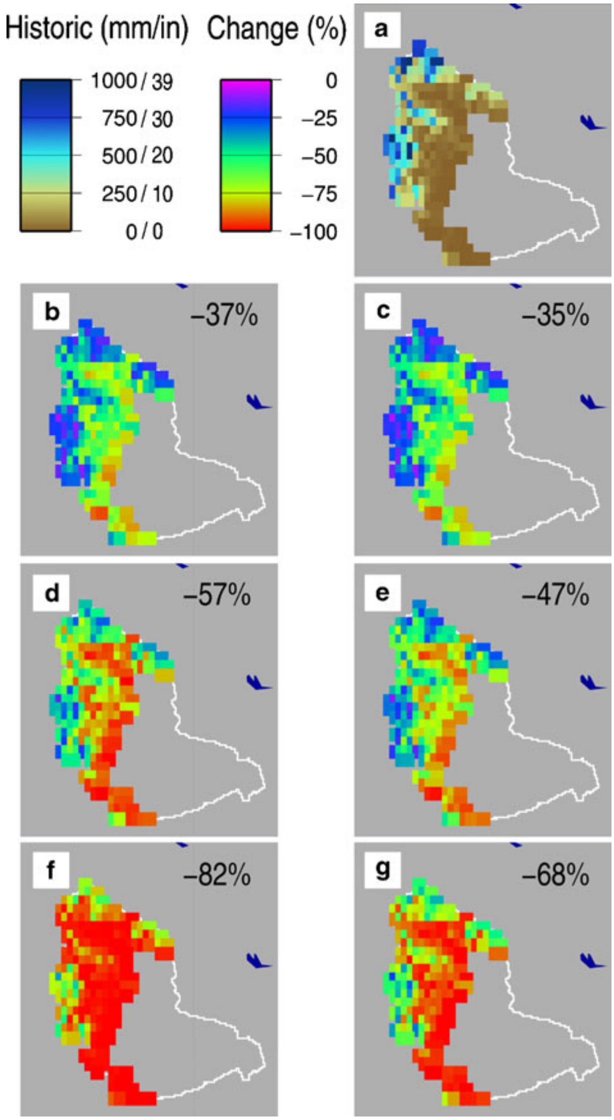

Fig. 13 Projected changes in April 1 SWE in the Yakima River watershed as simulated by the VIC model. **a** historical April 1 SWE (mean over water years 1917–2006). **b**, **c** Projected change in April 1 SWE for the 2020s (A1B and B1 SRES scenarios, respectively). **d**, **e** represent projected change in April 1 SWE for the 2040s (A1B and B1 SRES scenarios, respectively). **f**, **g** Projected change in April 1 SWE for the 2080s (A1B and B1 SRES scenarios, respectively). Percent change values represent spatially averaged April 1 SWE across the watershed with respect to the historical period

5 Conclusions and recommendations

Climate change will impact Washington State's hydrologic resources significantly over the next century. Sensitive areas, such as transient watersheds will experience substantial impacts by the 2020s. Annual runoff across the State is projected to change little by the 2020s (decrease of 0.1% to an increase of 2%), to increase by 2.2–2.7% by the 2040s, and increase by 4.2–6.4% by the 2080s. These changes are primarily driven by projected increases in winter precipitation. April 1 SWE is projected to decrease by an average of approximately 28–30% across the State by the 2020s, 38–46% by the 2040s and 56–70% by the 2080s, based on the composite changes in temperature and precipitation described by Mote and Salathé (2010). Soil moisture is projected to be in the 38th to 43rd percentile by the 2020s, 35th to 40th percentile by the 2040s, and 32nd to 35th percentile by the 2080s, with 50% being equal to mean historical values.

The effects of climate change on the urban water supply basins of Puget Sound and the agriculturally rich area of the Yakima watershed will be significant. In the watersheds of the Puget Sound, which are characterized as transient, snowpack is projected to decrease and seasonal streamflow is projected to shift from the characteristic double-peak to a single-peak, characteristic of rain-dominant watersheds. By the 2080s, April 1 snowpack in the watersheds will be almost entirely absent.

Projections of weekly SWE over the Yakima watershed indicate that SWE will decrease by an average of 39% by the 2020s, 50% by the 2040s, and 70% by the 2080s. The suite of projections for the 2020s indicate increased streamflow in winter but no significant change in the timing of the peak. Yet, by the 2040s, the spring peak streamflow is projected to shift toward a characteristic lower elevation transient watershed with two streamflow peaks (defined in Section 1). And by the 2080s, the streamflow regime will become rain dominant.

This study utilizes climate change projections from the full suite of 39 scenarios based on A1B and B1 SRES scenarios using a delta method approach. However, further refinement of the statistical downscaling of the transient daily climate change projections such that results from coupled hydrologic simulations are robust at sub-monthly time scales would be beneficial to evaluate the potential changes in the relative variability of temperature and precipitation and other related variables. The combination of spatial and temporal statistical downscaling can introduce unrealistic storm events in the future period. One possible method to eliminate this problem is to maintain the historic sequencing of daily variability in the transient scenarios through development of a hybrid of the delta method and BCSD approach. These climate change projections would provide a better understanding of the uncertainty of future climate and the variability of hydrologic processes. Barriers to widespread use of climate change projections in water resources studies include the availability of data and the knowledge to effectively and appropriately use this information for specific watershed studies. This study has attempted to clarify our understanding of projected hydrologic changes in Washington and, along with companion papers in this special issue, provide a framework for future studies in other regions. The ability to educate the public about the implications of climate change is crucial, as the climate system clearly is non-stationary, and as Milly et al. (2008) have argued, traditional methods that rely on historical information alone to plan for the future are no longer defensible.

Acknowledgements The authors thank Shraddhanand Shukla at the University of Washington and Andrew Wood of 3Tier for their consultation with respect to the 1/16th degree VIC model calibration and implementation. We also thank Tazebe Kiros Beyene and Elizabeth Clark at the University of Washington for their assistance with data analysis and troubleshooting, and Robert Norheim at the University of Washington Climate Impacts Group for his assistance with data analysis and graphics. Finally, we thank four anonymous reviewers who provided helpful comments that improved the manuscript. This publication is part of the Washington Climate Change Impacts Assessment, funded by the 2007 Washington State Legislature through House Bill 1303. This publication is partially funded by the NOAA Regional Integrated Sciences and Assessments program and the NOAA Climate Dynamics and Experimental Prediction/Applied Research Centers program under NOAA Cooperative Agreement No. NA17RJ1232 to the Joint Institute for the Study of the Atmosphere and Ocean (JISAO). This is JISAO Contribution #1788.

References

Alberti M, Weeks R, Coe S (2004) Urban land-cover change analysis in central Puget Sound. Photogramm Eng Remote Sensing 70:1043–1052

Andreadis K, Storck P, Lettenmaier DP (2009) Modeling snow accumulation and ablation processes in forested environments. Water Resour Res 45:W05429. doi:10.1029/2008WR007042

Barnett TP, Adam JC, Lettenmaier DP (2005) Potential impacts of a warming climate on water availability in snow-dominated regions. Nature 438:303–309

Barnett TP, Pierce DW, Hidalgo HG, Bonfils C, Santer BD, Das T, Bala G, Wood AW, Nozawa T, Mirin AA, Cayan DR, Dettinger MD (2008) Human-induced changes in the hydrology of the western United States. Science 319(5866):1080–1083

Beven KJ, Kirkby MJ (1979) A physically based, variable contributing area model of basin hydrology. Hydrol Sci Bull 24(1):43–69

Bowling LC, Lettenmaier DP (2001) The effects of forest roads and harvest on catchment hydrology in a mountainous maritime environment. In: Wigmosta MS, Burges SJ (eds) Land use and watersheds: human influence on hydrology and geomorphology in urban and forest areas, AGU Water Sci Appl, vol 2, pp 145–164

Bowling LC, Storck P, Lettenmaier DP (2000) Hydrologic effects of logging in western Washington, United States. Wat Resour Res 36:3223–3240

Brekke LD, Miller NL, Bashford KE, Quinn NWT, Dracup JA (2004) Climate change impacts uncertainty for water resources in the San Joaquin river basin, California. J Am Water Resour Assoc 40(1):149–164

Casola JH, Kay JE, Snover AK, Norheim RA, Whitely Binder LC, Climate Impacts Group (2005) Climate impacts on Washington's hydropower, water Supply, forests, fish, and agriculture. A report prepared for King County (Washington) by the Climate Impacts Group, Center for Science in the Earth System, Joint Institute for the Study of the Atmosphere and Ocean, University of Washington, Seattle

Cherkauer KA, Bowling LC, Lettenmaier DP (2003) Variable Infiltration Capacity (VIC) cold land process model updates. Glob Planet Change 38(1–2):151–159

Christensen N, Lettenmaier DP (2007) A multimodel ensemble approach to assessment of climate change impacts on the hydrology and water resources of the Colorado River basin. Hydrol Earth Syst Sci 11:1417–1434

Christensen NS, Wood AW, Voisin N, Lettenmaier DP, Palmer RN (2004) The effects of climate change on the hydrology and water resources of the Colorado River basin. Clim Change 62: 337–363

Cuo L, Lettenmaier DP, Mattheussen BP, Storck P, Wiley M (2008) Hydrological prediction for urban watersheds with the distributed hydrology–soil–vegetation model. Hydrol Process 22(21):4205–4213

Cuo L, Lettenmaier DP, Alberti M, Richey JE (2009) Effects of a century of land cover and climate change on the hydrology of Puget Sound basin. Hydrol Process 23:907–933

Daly C, Neilson RP, Phillips DL (1994) A statistical–topographic model for mapping climatological precipitation over mountainous terrain. J Appl Meteorol 33:140–158

Daly C, Gibson WP, Taylor G, Johnson GL, Pasteris P (2002) A knowledge-based approach to the statistical mapping of climate. Clim Res 22:99–113

Dooge JC (1992) Hydrologic models and climate change. J Geophys Res 97(D3):2677–2686

Easterling DR, Horton B, Jones PD, Peterson TC, Karl TR, Parker DE, Salinger MJ, Razuvayev V, Plummer N, Jamason P, Folland CK (1997) Maximum and minimum temperature trends for the globe. Science 18:364–367

Economic and Engineering Services, Inc (2003) Watershed management plan, Yakima River basin. For Yakima River watershed planning unit and Tri-County water resources agency

Hamlet AF, Lettenmaier DP (1999) Effects of climate change on hydrology and water resources of the Columbia River basin. J Am Water Resour Assoc 35:1597–1624

Hamlet AF, Lettenmaier DP (2005) Production of temporally consistent gridded precipitation and temperature fields for the continental United States. J Hydrometeorol 6:330–336

Hamlet AF, Lettenmaier DP (2007) Effects of 20th century warming and climate variability on flood risk in the western US. Water Resour Res 43:W06427

Hamlet AF, Mote PW, Clark M, Lettenmaier DP (2005) Effects of temperature and precipitation variability on snowpack trends in the western United States. J Clim 18(21):4545–4561

Hamlet AF, Lee SY, Mickelson KEB, Elsner MM (2010) Effects of projected climate change on energy supply and demand in the Pacific Northwest and Washington State. Clim Change. doi:10.1007/s10584-010-9857-y
Hayhoe K, Wake C, Huntington TG, Luo L, Schwartz MD, Sheffield J, Wood EF, Anderson B, Bradbury J, DeGaetano TT, Wolfe D (2007) Past and future changes in climate and hydrological indicators in the US Northeast. Clim Dyn 28:381–407
IPCC (1995) IPCC Second assessment: report of working group I - the science of climate change, with a Summary for Policymakers (SPM). In: Houghton JT, Meira Filho MG, Callender BA, Harris N, Kattenberg A, Maskell K (eds). Cambridge University Press, UK, 572 pp
IPCC (2001) Climate change 2001: the scientific basis. In: Houghton JT, Ding Y, Griggs DJ, Noguer M, van der Linden PJ, Dai X, Maskell K, Johnson CA (eds) Contribution of working group I to the third assessment report of the intergovernmental panel on climate change. Cambridge University Press, Cambridge, 881 pp
IPCC (2007) Summary for policymakers. In: Solomon S, Qin D, Manning M, Chen Z, Marquis M, Averyt KB, Tignor M, Miller HL (eds) Climate change 2007: the physical science basis. Contribution of working group I to the fourth assessment report of the intergovernmental panel on climate change. Cambridge University Press, Cambridge
Kalaney E et al (1996) The NCEP/NCAR 40-year reanalysis project. Bull Am Meteorol Soc 77:437–471
Lamarche J, Lettenmaier DP (2001) Effects of forest roads on flood flows in the Deschutes River basin, Washington. Earth Surf Process Landf 26:115–134
Lettenmaier DP, Wood AW, Palmer RN, Wood EF, Stakhiv EZ (1999) Water resources implications of global warming: a U.S. regional perspective. Clim Change 43(3):537–579
Leung LR, Wigmosta MS, Ghan SJ, Epstein DJ, Vail LW (1996) Application of a subgrid orographic precipitation/surface hydrology scheme to a mountain watershed. J Geophys Res 101(D8):12803–12817
Liang X, Lettenmaier DP, Wood EF, Burges SJ (1994) A simple hydrologically based model of land surface water and energy fluxes for GSMs. J Geophys Res 99(D7):14,415–14,428
Liang X, Wood EF, Lettenmaier DP (1996) Surface soil moisture parameterization of the VIC-2L model: evaluation and modifications. Glob Planet Change 13:195–206
Liang X, Wood EF, Lohmann D, Lettenmaier DP and others (1998) The project for intercomparison of land-surface parameterization schemes (PILPS) phase-2c Red-Arkansas River basin experiment: 2. Spatial and temporal analysis of energy fluxes. J Glob Planet Change 19:137–159
Littell JS, Oneil EE, McKenzie D, Hicke JA, Lutz J, Norheim RA, Elsner MM (2010) Forest ecosystems, disturbance, and climatic change in Washington State, USA. Clim Change. doi: 10.1007/s10584-010-9858-x
Mantua N, Tohver IM, Hamlet AF (2010) Climate change impacts on streamflow extremes and summertime stream temperature and their possible consequences for freshwater salmon habitat in Washington State. Clim Change. doi:10.1007/s10584-010-9845-2
Matheussen B, Kirschbaum RL, Goodman IA, O'Donnell GM, Lettenmaier DP (2000) Effects of land cover change on streamflow in the interior Columbia basin. Hydrol Process 14(5):867–885
Maurer EP (2007) Uncertainty in hydrologic impacts of climate change in the Sierra Nevada, California under two emissions scenarios. Clim Change 82(3–4):309–325
Maurer EP, Duffy PB (2005) Uncertainty in projections of streamflow changes due to climate change in California. Geophys Res Lett 32(3):L03704
Maurer EP, Wood AW, Adam JC, Lettenmaier DP, Nijssen B (2002) A long-term hydrologically based dataset of land surface fluxes and states for the conterminous United States. J Clim 15:3237–3251
Meehl GA, Stocker TF, Collins WD, Friedlingstein P, Gaye AT, Gregory JM, Kitoh A, Knutti R, Murphy JM, Noda A, Raper SCB, Watterson IG, Weaver AJ, Zhao Z-C (2007) Global climate projections. In: Solomon S, Qin D, Manning M, Chen Z, Marquis M, Averyt KB, Tignor M, Miller HL (eds) Climate change 2007: the physical science basis. Contribution of working group I to the fourth assessment report of the intergovernmental panel on climate change. Cambridge University Press, Cambridge
Miller NL, Bashford KE, Strem E (2003) Potential impacts of climate change on California hydrology. J Am Water Resour Assoc 39:771–784
Milly PCD, Dunne KA, Vecchia AV (2005) Global pattern of trends in streamflow and water availability in a changing climate. Nature 438:347–350
Milly PCD, Betancourt J, Falkenmark M, Hirsch RM, Kundzewicz ZW, Lettenmaier DP, Stouffer RJ (2008) Stationarity is dead: whither water management. Science 319:573–574

Mote PW (2006) Climate-driven variability and trends in mountain snowpack in western North America. J Clim 19(23):6209–6220

Mote PW, Salathé EP Jr (2010) Future climate in the Pacific Northwest. Clim Change. doi: 10.1007/s10584-010-9848-z

Mote PW, Hamlet AF, Clark M, Lettenmaier DP (2005) Declining mountain snowpack in western North America. Bull Am Meteorol Soc 86(1):39–49

Nakićenović N, Swart R (eds) (2000) Special report on emissions scenarios. A special report of working group III of the intergovernmental panel on climate change. Cambridge University Press, Cambridge, United Kingdom and New York, NY, USA, 599

Nash LL, Gleick PH (1991) The sensitivity of streamflow in the Colorado Basin to climatic changes. J Hydrol 125:221–241

Nijssen BN, Lettenmaier DP, Liang X, Wetzel SW, Wood EF (1997) Streamflow simulation for continental-scale river basins. Water Resour Res 33(4):711–724

Nijssen BN, O'Donnell GM, Lettenmaier DP, Lohmann D, Wood EF (2001) Predicting the discharge of global rivers. J Clim 14:3307–3323

Payne JT, Wood AW, Hamlet AF, Palmer RN, Lettenmaier DP (2004) Mitigating the effects of climate change on the water resources of the Columbia River basin. Clim Change 62:233–256

Refsgaard JC, Storm S (1996) Distributed hydrologic modeling. Chapter 3: construction, calibration, and validation of hydrological models. Kluwer Academic Publishers

Salathé EP, Mote PW, Wiley MW (2007) Review of scenario selection and downscaling methods for the assessment of climate change impacts on hydrology in the United States Pacific Northwest. Int J Climatol 27(12):1611–1621

Salathé EP Jr, Leung LR, Qian Y, Zhang Y (2010) Regional climate model projections for the State of Washington. Clim Change. doi:10.1007/s10584-010-9849-y

Sankarasubramanian A, Vogel RM, Limbrunner JF (2001) Climate elasticity of streamflow in the United States. Water Resour Res 37(6):1771–1781

Schaake JC (1990) From climate to flow. In: Waggoner PE (ed) Climate change and US water resources. John Wiley, New York, pp 177–206

Shepard DS (1984) Computer mapping: the SYMAP interpolation algorithm. In: Willmott GL, Reidel CJ (eds) Spatial statistics and Models Gaille, pp 133–145

Snover AK, Hamlet AF, Lettenmaier DP (2003) Climate change scenarios for water planning studies: pilot applications in the Pacific Northwest. Bull Am Meteorol Soc 84(11):1513–1518

Stewart IT, Cayan DR, Dettinger MD (2005) Changes toward earlier streamflow timing across western North America. J Clim 18:1136–1155

Vano JA, Voisin N, Cuo L, Hamlet AF, Elsner MM, Palmer RN, Polebitski A, Lettenmaier DP (2010a) Climate change impacts on water management in the Puget Sound region, Washington State, USA. Clim Change. doi:10.1007/s10584-010-9846-1

Vano JA, Voisin N, Scott M, Stöckle CO, Hamlet AF, Mickelson KEB, Elsner MM, Lettenmaier DP (2010b) Climate change impacts on water management and irrigated agriculture in the Yakima River Basin, Washington, USA. Clim Change. doi:10.1007/s10584-010-9856-z

Van Rheenen NT, Wood AW, Palmer RN, Lettenmaier DP (2004) Potential implications of PCM climate change scenarios for California hydrology and water resources. Clim Change 62: 257–281

VanShaar JR, Haddeland I, Lettenmaier DP (2002) Effects of land cover changes on the hydrologic response of interior Columbia River Basin forested catchments. Hydrol Process 16(13):2499–2520

Vicuna S, Maurer EP, Joyce B, Dracup JA, Purkey D (2007) The sensitivity of California water resources to climate change scenarios. J Am Water Res Assoc 43(2):482–498

Wang A, Bohn TJ, Mahanama SP, Koster RD, Lettenmaier DP (2009) Multimodel ensemble reconstruction of drought over the continental United States. J Clim 22:2694–2712

Wigmosta MS, Lettenmaier DP (1999) A comparison of simplified methods for routing topographically driven subsurface flow. Water Resour Res 35(1):255–264

Wigmosta MS, Vail LW, Lettenmaier DP (1994) A distributed hydrology: vegetation model for complex terrain. Can J For Res 30:1665–1679

Wood AW, Maurer EP, Kumar A, Lettenmaier DP (2002) Long range experimental hydrologic forecasting for the eastern US. J Geophys Res 107(D20):4429

Wood AW, Leung LR, Sridhar V, Lettenmaier DP (2004) Hydrologic implications of dynamical and statistical approaches to downscaling climate model outputs. Clim Change 62(1–3):189–216